ULTRALUMINOUS INFRARED GALAXIES AND THE ORIGIN OF QUASARS

D. B. SANDERS,[1] B. T. SOIFER,[1] J. H. ELIAS,[1] B. F. MADORE,[1,2,3] K. MATTHEWS,[1]
G. NEUGEBAUER,[1] AND N. Z. SCOVILLE[4]
Received 1987 May 7; accepted 1987 July 1

ABSTRACT

An evolutionary connection between ultraluminous infrared galaxies and quasars is deduced from the observations of all 10 infrared galaxies with luminosities $L(8–1000 \ \mu m) \geq 10^{12} \ L_\odot$, taken from a flux-limited sample of infrared bright galaxies. Images of the infrared galaxies show that nearly all are strongly interacting merger systems with exceptionally luminous nuclei. Millimeter-wave CO observations show that these objects typically contain $0.5–2 \times 10^{10} \ M_\odot$ of H_2. Optical spectra indicate a mixture of starburst and active galactic nucleus (AGN) energy sources, both of which are apparently fueled by the tremendous reservoir of molecular gas. It is proposed that these ultraluminous infrared galaxies represent the initial, dust-enshrouded stages of quasars. Once these nuclei shed their obscuring dust, allowing the AGN to visually dominate the decaying starburst, they become optically selected quasars. The origin of quasars through the merger of molecular gas-rich spiral galaxies can account for both the increased number of high-luminosity quasars at large redshift, when the universe was smaller and gas supplies less depleted, and the observed "redshift-cutoff" of quasars which represents the epoch after galaxy formation when the first collisions occur.

Subject headings: galaxies: evolution — galaxies: photometry — infrared: sources — quasars

I. INTRODUCTION

One of the most important results of the *IRAS* survey has been the discovery of a significant number of galaxies having luminosities $> 10^{12} \ L_\odot$ which emit the bulk of their energy at infrared wavelengths (Houck *et al.* 1984, 1985; Soifer *et al.* 1984*a, b*). At bolometric luminosities above $10^{10} \ L_\odot$ (in this paper we adopt $H_0 = 75$ km s^{-1} Mpc^{-1}) the space density of infrared galaxies in the local universe ($z \lesssim 0.1$) is comparable to, or greater than, that for active and starburst galaxies (Soifer *et al.* 1986). Even at the highest luminosities, the "ultraluminous" galaxies with infrared luminosities[5] above $10^{12} \ L_\odot$ are more numerous than optically selected quasars.

We have undertaken a major program of optical, near-infrared, and millimeter-wave observations of the ultraluminous infrared galaxies in an attempt to understand both the nature of the host galaxy and the origin of the greatly enhanced infrared radiation. This program is part of a larger study of all the galaxies in the *IRAS* Bright Galaxy Survey (Sanders *et al.* 1987*c*). The *IRAS* Bright Galaxy Sample includes all extragalactic objects brighter than 5.4 Jy at 60 μm with Galactic latitude $|b| > 30°$ and with declination $\delta > -30°$. Because these are the brightest galaxies in the sky at 60 μm, this sample represents the best opportunity for the study of the infrared emission processes in galaxies. A complete description of the Bright Galaxy Survey and the luminosity function for these galaxies is given in Soifer *et al.* (1986, 1987). A preliminary description of the morphology and molecular gas content of *IRAS* galaxies with infrared luminosities $10^{11}–10^{12} \ L_\odot$ is given in Sanders *et al.* (1986).

The data for the ultraluminous infrared galaxies are presented in § II. In § III the properties of the ultraluminous galaxies—morphology, spectral classification, energy distribution, and gas content—are discussed, and in § IV a model for the origin and evolution of ultraluminous infrared galaxies is presented.

II. OBSERVATIONS

a) The Ultraluminous IRAS Galaxy Sample

The *IRAS* Bright Galaxy Survey covered $\sim 14,500$ deg^2 and included 324 galaxies brighter than 5.4 Jy at 60 μm. The maximum redshift of a sample galaxy is 0.081. Three percent of the sample, or 10 galaxies, have infrared luminosities larger than $10^{12} \ L_\odot$; these are listed in Table 1 along with the measured redshifts, infrared flux densities, and the computed infrared luminosities. The majority of these 10 galaxies have blue magnitudes fainter than 15.5 mag, hence they are not found in the standard catalogs. The redshifts for most of the ultraluminous galaxies have been taken from a recent CO(1 → 0) emission-line survey of galaxies in the *IRAS* Bright Galaxy Sample (Sanders, Scoville, and Soifer 1987). The redshifts for *IRAS* 08572+3915, *IRAS* 09320+6134, and *IRAS* 15250+3609 were obtained with the double spectrograph (Oke and Gunn 1982) on the Hale 5 m telescope of the Palomar Observatory. The mean redshift for the ultraluminous sample is $z = 0.055$. The sample of objects listed in Table 1, although relatively small, is an impressive number when one realizes that the only other known objects in the same volume of space of comparable luminosity are quasars, of which there are less than half as many.

The minimum luminosity for defining the ultraluminous sample was chosen to correspond to the maximum luminosity bin (log $[L/L_\odot] = 12–12.5$) of galaxies in the *IRAS* Bright Galaxy Survey that was used by Soifer *et al.* (1987) to determine the luminosity function of infrared galaxies. More important, however, is the fact that $10^{12} \ L_\odot$ is equivalent to the generally accepted minimum bolometric luminosity of quasars (Schmidt and Green 1983; Véron-Cetty and Véron 1983).

---

[1] Palomar Observatory, California Institute of Technology.

[2] Killam Fellow, Canada Council 1986–1988.

[3] Also at the David Dunlap Observatory, University of Toronto.

[4] Owens Valley Radio Observatory, California Institute of Technology.

[5] Throughout this paper, unless otherwise indicated, infrared luminosity refers to $L(8–1000 \ \mu m)$ which has been computed from the *IRAS* data as discussed in § II*b*.

TABLE 1

ULTRALUMINOUS *IRAS* GALAXIES IN THE *IRAS* BRIGHT GALAXY SAMPLE

| IRAS (Other) | cZ^a (km s^{-1}) | F_ν (Jy)[b] | | | | $\log[L(8\text{–}1000\ \mu m)/L_\odot]$ |
		12 μm	25 μm	60 μm	100 μm	
05189−2524	12,816	0.76	3.52	13.94	11.68	12.10
08572+3915	17,480	0.35	1.73	7.53	4.59	12.09
09320+6134 .... (UGC 05101)	12,000	0.25	1.05	12.09	20.07	12.01
12112+0305	21,788	<0.18	0.63	8.36	9.91	12.29
12540+5708 .... (Mrk 231)	12,660	1.81	8.52	33.60	30.89	12.52
13428+5608 .... (Mrk 273)	11,132	0.31	2.33	23.70	22.31	12.14
14348−1447	24,732	0.09	0.56	6.82	7.49	12.29
15250+3609	16,000	0.15	1.32	7.50	5.86	12.00
15327+2340 .... (Arp 220)	5450	0.46	8.11	104.08	117.69	12.19
22491−1808	23,170	<0.12	0.57	5.54	4.64	12.13

NOTE.—Objects in the *IRAS* Bright Galaxy Survey (Soifer *et al.* 1986, 1987) with $L(8\text{–}1000\ \mu m) \geq 10^{12}\ L_\odot$.

[a] Mean heliocentric redshift. For *IRAS* 08572+3915, *IRAS* 09320+6134, and *IRAS* 15250+3609 the redshift is determined from an optical spectrum and has an uncertainty of ± 100 km s^{-1}. In all other cases the redshift is taken from CO($J = 1 \rightarrow 0$) data and has an uncertainty of ± 20 km s^{-1}.

[b] *IRAS* flux densities from co-added survey scans.

b) Infrared Luminosities

The *IRAS* flux densities listed in Table 1 were determined from co-addition of all survey data rather than simply taken from the *IRAS Point Source Catalog* (1985, hereafter the PSC). The resulting enhanced sensitivity leads to the detection of several sources at 12 μm and allows a more accurate determination of the far-infrared color temperatures, but has little effect on the computed total far-infrared luminosity. The tabulated luminosity was computed using the prescription outlined by Perault *et al.* (1986) which employs data from all four *IRAS* bands to approximate $L(8\text{–}1000\ \mu m)$. Since several of the ultraluminous objects emit a significant proportion of their infrared luminosity shortward of 40 μm, this method provides a significantly better approximation to the total infrared luminosity than the more commonly used $L_{\rm fir}$, determined by fitting a single-temperature dust model to the 60 μm and 100 μm observations according to the prescription given in *Cataloged Galaxies and Quasars Detected in the IRAS Survey* (1985).

c) Imaging

It was possible to identify all of the infrared objects included in Table 1 with an optical counterpart on the Palomar Sky Survey (POSS). All but one of the optical images were clearly extended, having diameters between 15″ and 40″ as measured on the red prints. The one exception was the starlike object *IRAS* 05189−2524. Seven of the 10 ultraluminous objects appeared to be peculiar galaxies, being either mergers or distorted systems with distinct wisps and tails.

Low-resolution images of the 10 ultraluminous objects, taken with the Palomar 1.5 m telescope showed that at least five were double galaxies which appeared to be partially merged. All of the ultraluminous galaxies were subsequently imaged at higher resolution, either with the "four-shooter" CCD camera on the Palomar 5 m telescope, or with the CCD direct image camera on the Palomar 1.5 m telescope as summarized in Table 2. Figure 1 shows all 10 images in contour form. Gray-scale images of each object are presented in Figures 2–11 (Plates 9–18). Descriptions of each object are given in Appendix A.

The contour maps (Fig. 1) and optical images (Figs. 2–11) show that all of the ultraluminous infrared galaxies have large-scale peculiar structures; most common are double jets, or tails, and in two cases, large rings are observed. Four objects also clearly have double nuclei. The image of Markarian 231 has previously been discussed by Sanders *et al.* (1987a), who

TABLE 2

OPTICAL IMAGING[a]

| IRAS	Telescope (m)	Resolution (″/pix)	Exposure (s)	Comments
05189−2524........	1.5	0.47	6000	Double tails
08572+3915........	5	0.34	300	Double nucleus
09320+6134........	5	0.34	300	Ring + jet
12112+0305........	5	0.34	300	Double nucleus
12540+5708........	1.5	0.47	2800	Double tails
13428+5608........	1.5	0.47	1200	"Triple nucleus" + jet
14348−1447........	1.5	1.29	300	Double nucleus
15250+3609........	1.5	0.47	900	Ring + small jet
15327+2340........	5	0.34	300	Double tails
22491−1808........	1.5	0.47	1200	Double tails

[a] 6500 Å (Gunn *r*).

PLATE 9
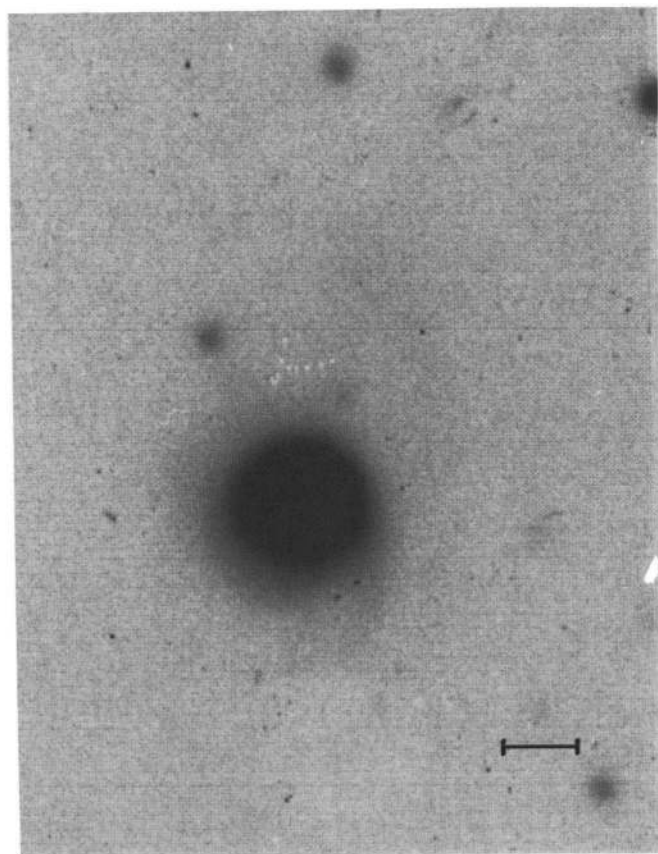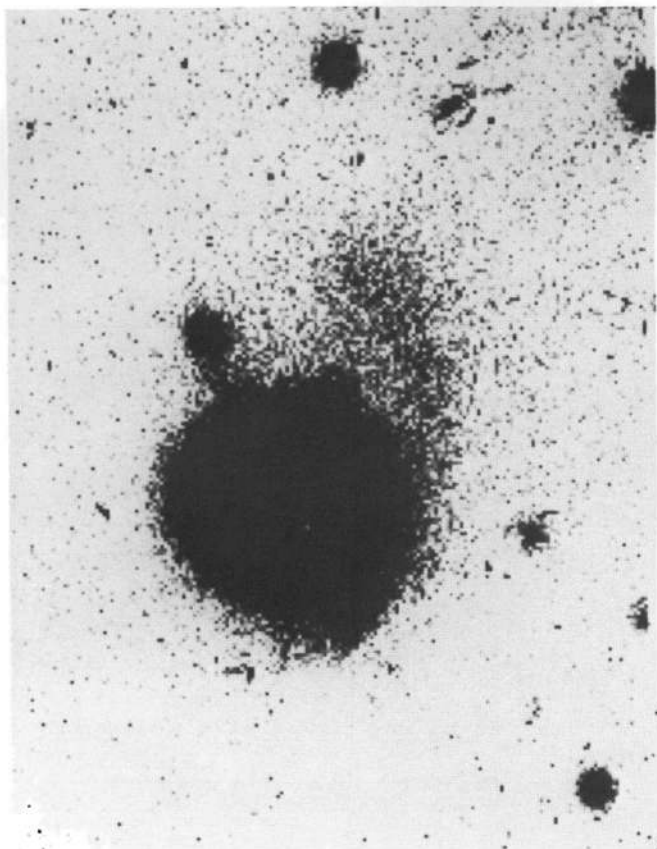
FIG. 2.—CCD images at 6500 Å (Gunn *r*) of the ultraluminous infrared galaxy *IRAS* 05189−2524. For all plots, north is at the top, and east is to the left. The scale is ∼0″.5 per pixel, and seeing was 1″–2″. Two stretches of the same image are presented to show both the nuclear structure and faint large-scale wisps and tails. Bar at the lower right represents 10″.
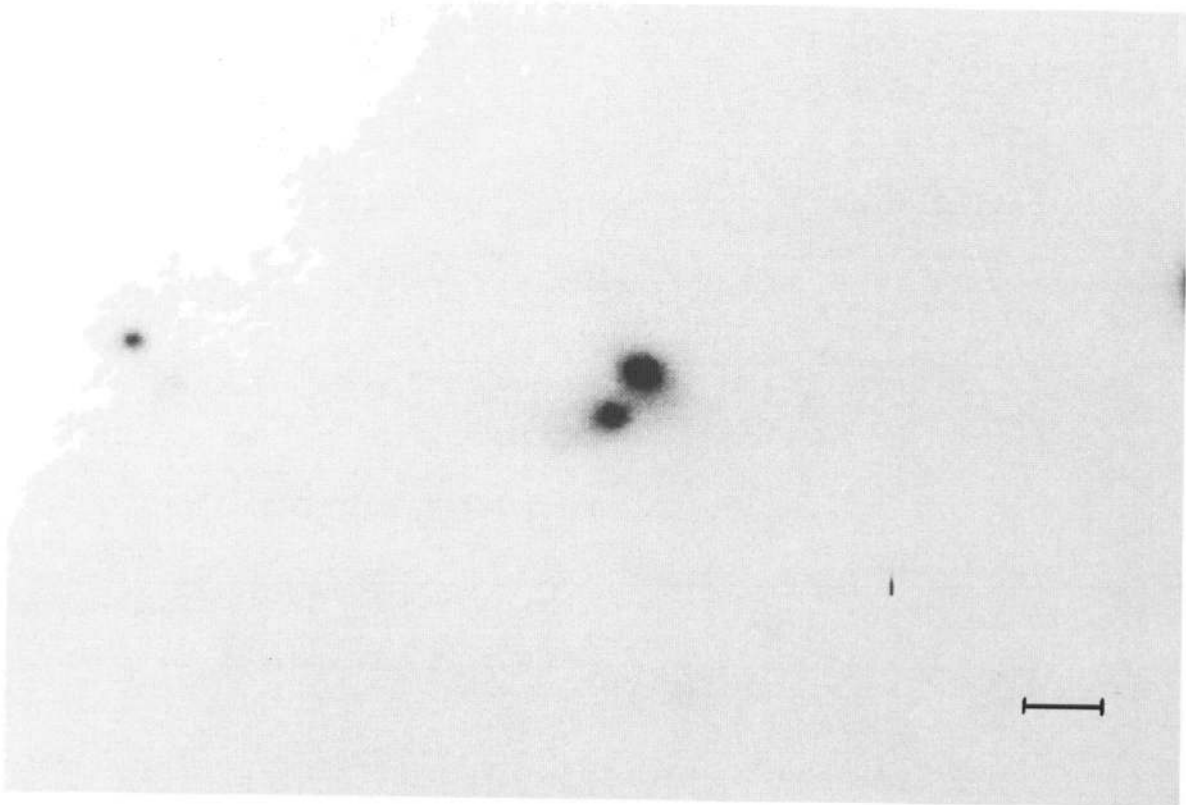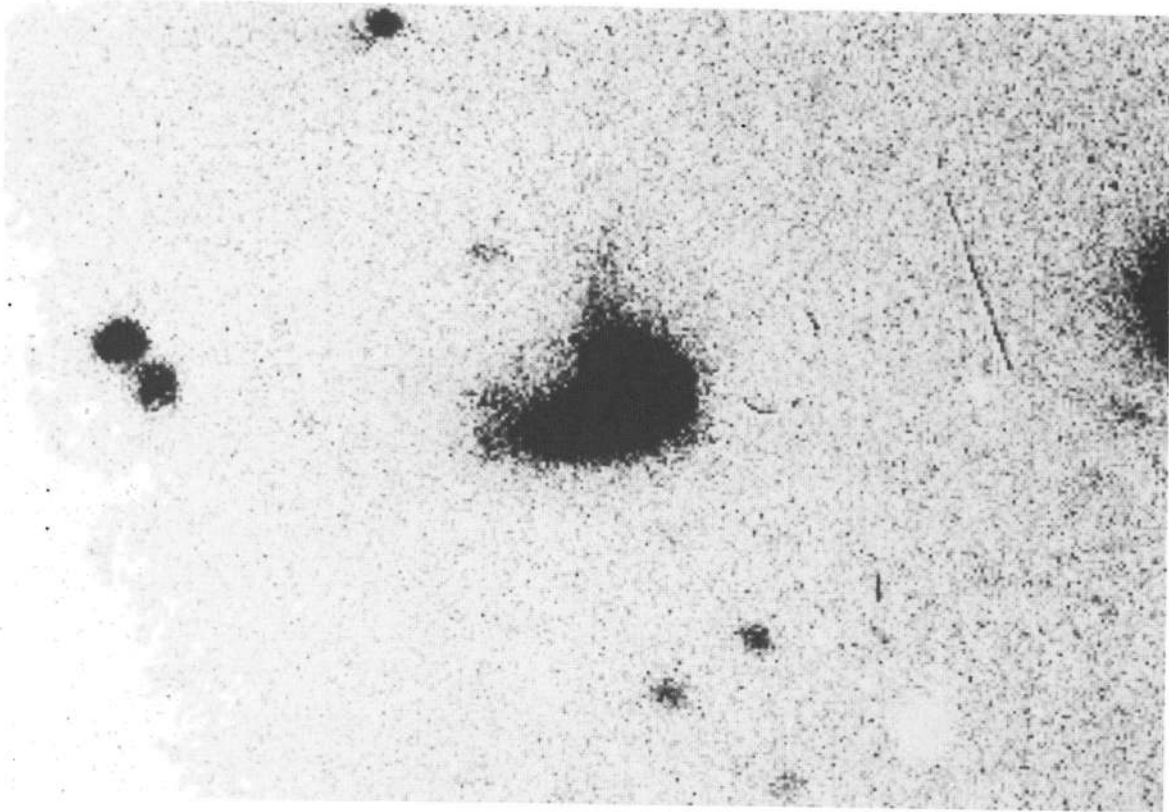
SANDERS *et al.* (*see* **325**, 75)

PLATE 10

FIG. 3.—*IRAS* 08572 + 3915
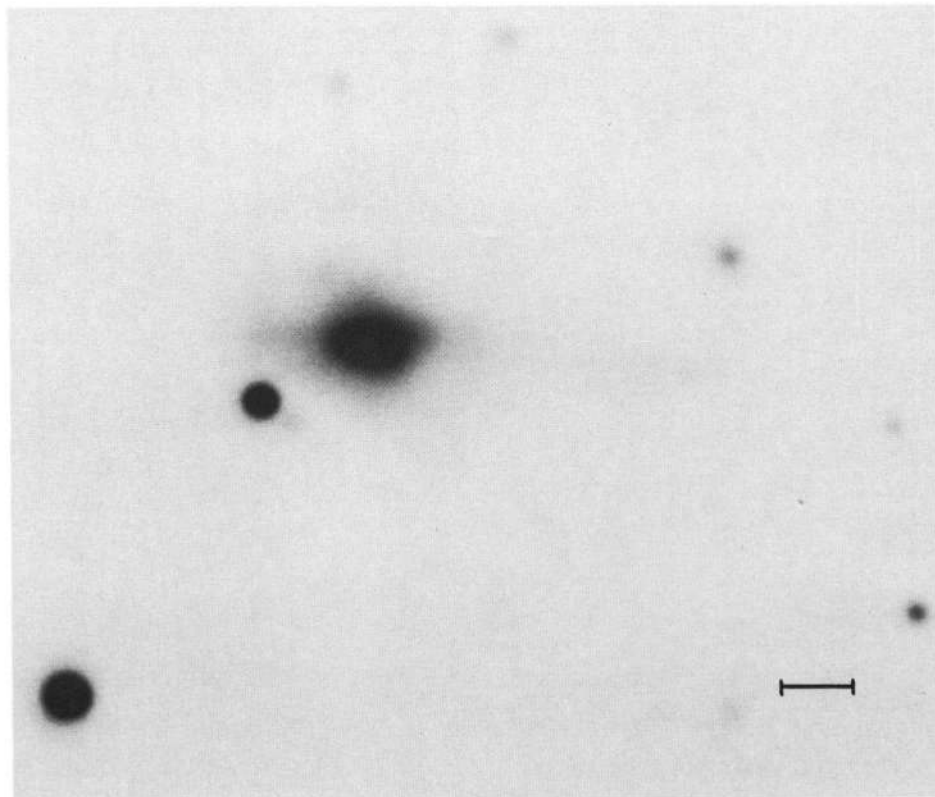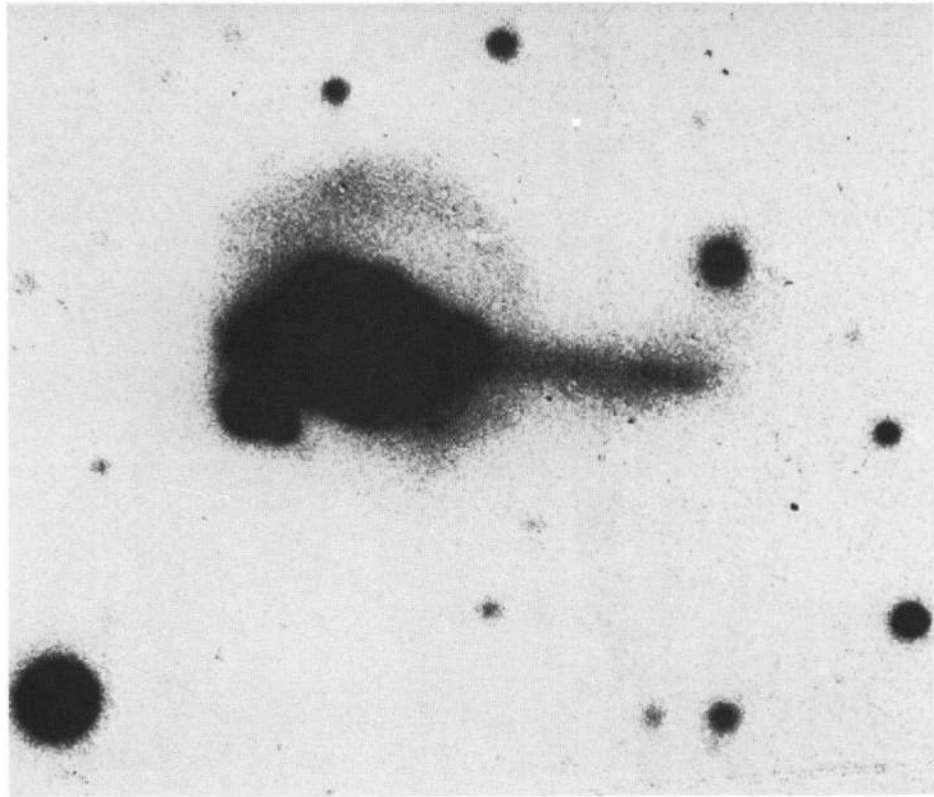
PLATE 11

Fig. 4.—*IRAS* 09320+6134 = UGC 05101
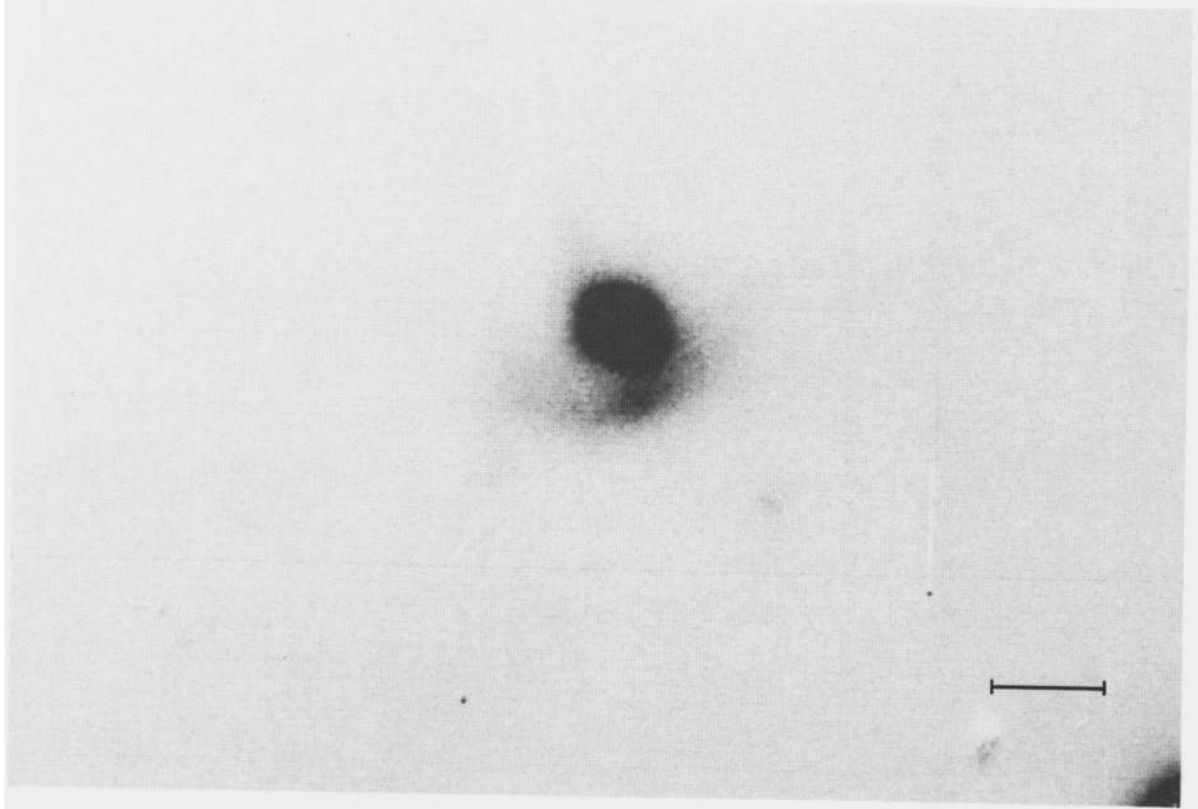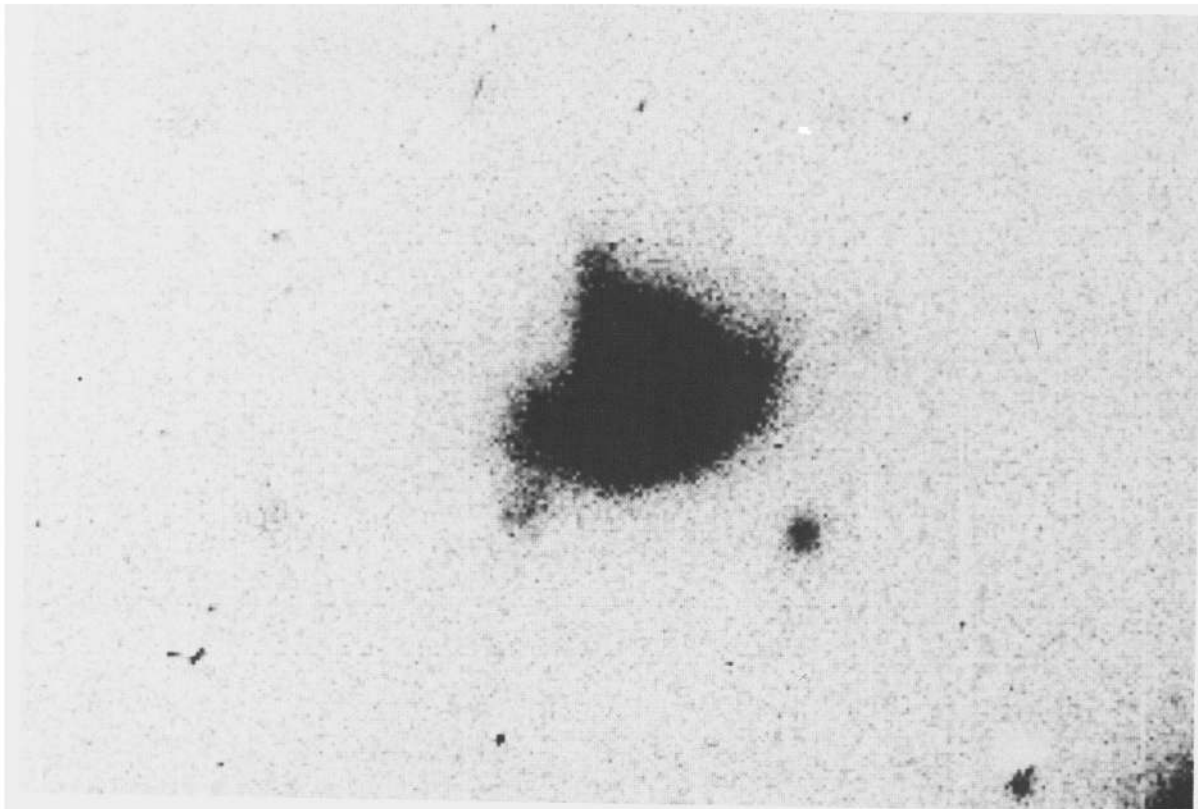
Fig. 5.—*IRAS* 12112+0305

PLATE 13

FIG. 6.—*IRAS* 12540 + 5708 = Markarian 231

SANDERS *et al.* (*see* **325**, 75)
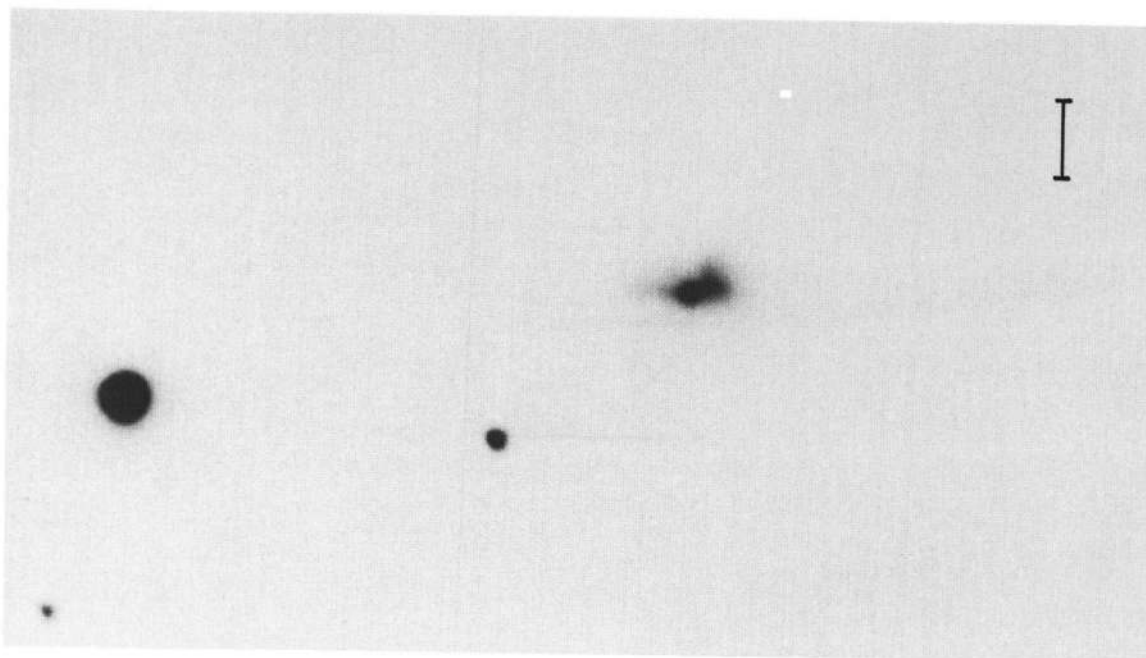
FIG. 7.—*IRAS* 13428 + 5608 = Markarian 273
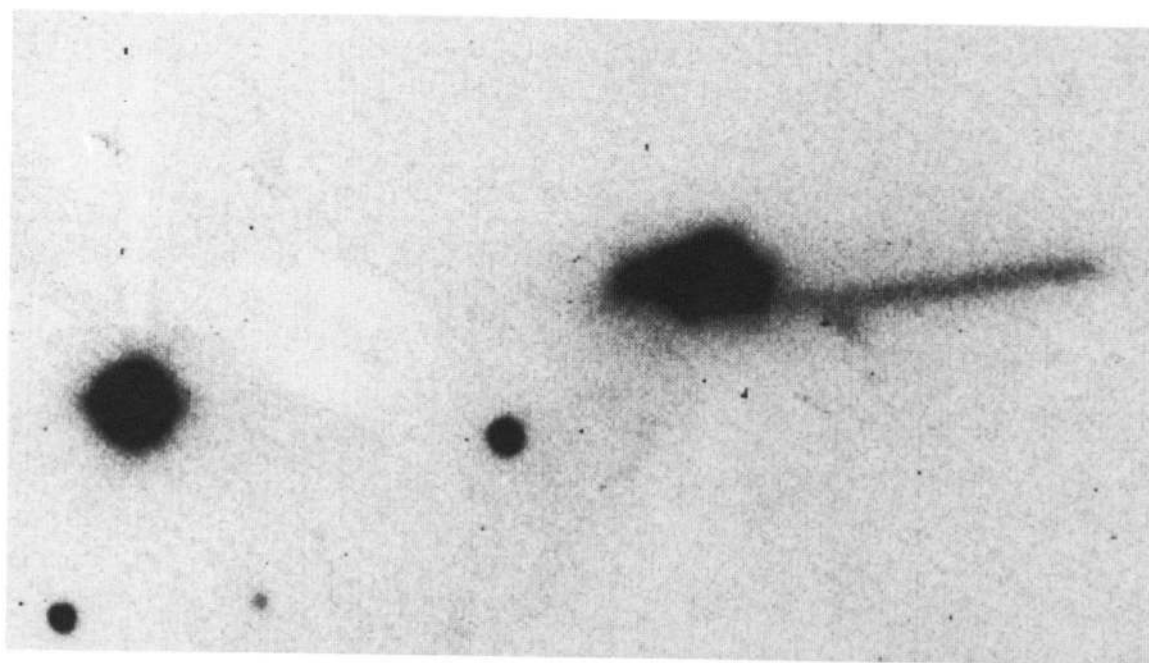
SANDERS *et al.* (*see* **325**, 75)
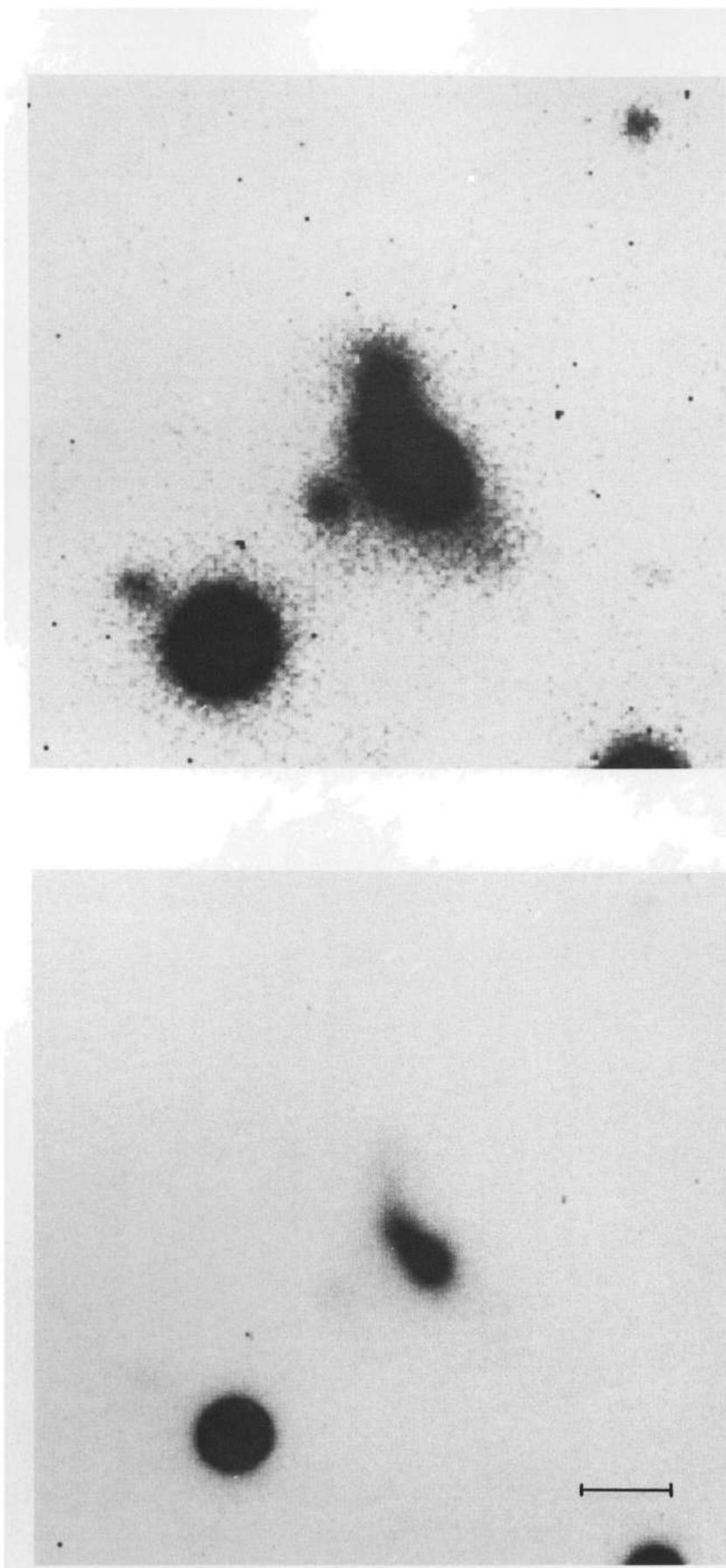
PLATE 15

Fig. 8.—*IRAS* 14348 − 1447
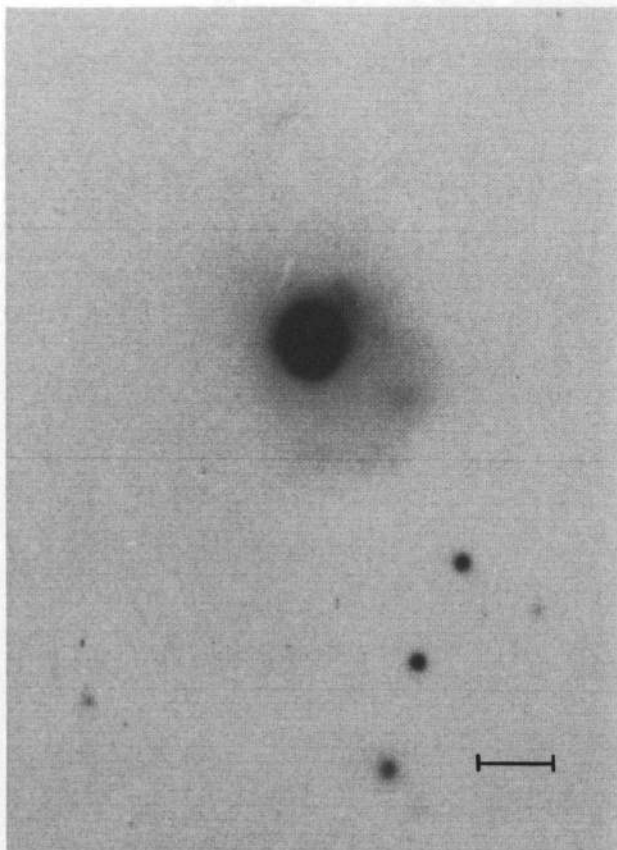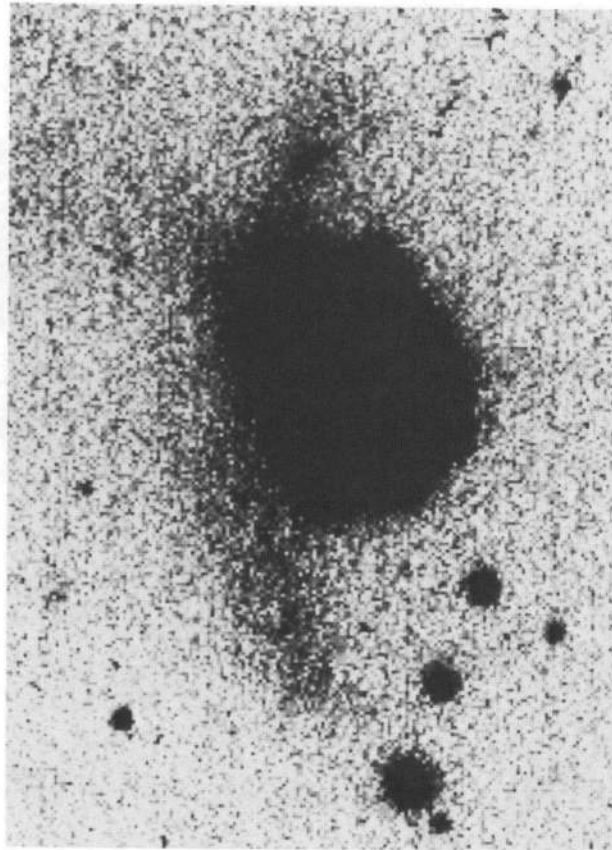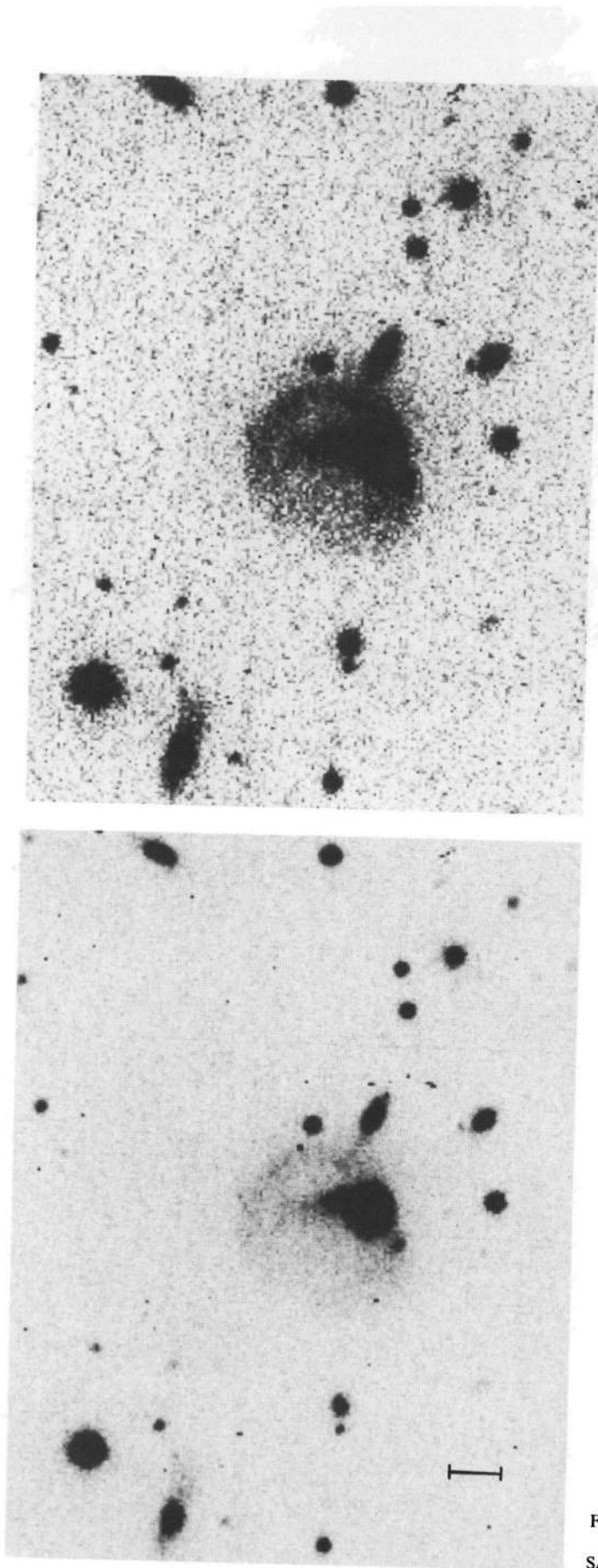
FIG. 9.—*IRAS* 15250+3609

SANDERS *et al.* (*see* **325**, 75)

PLATE 17
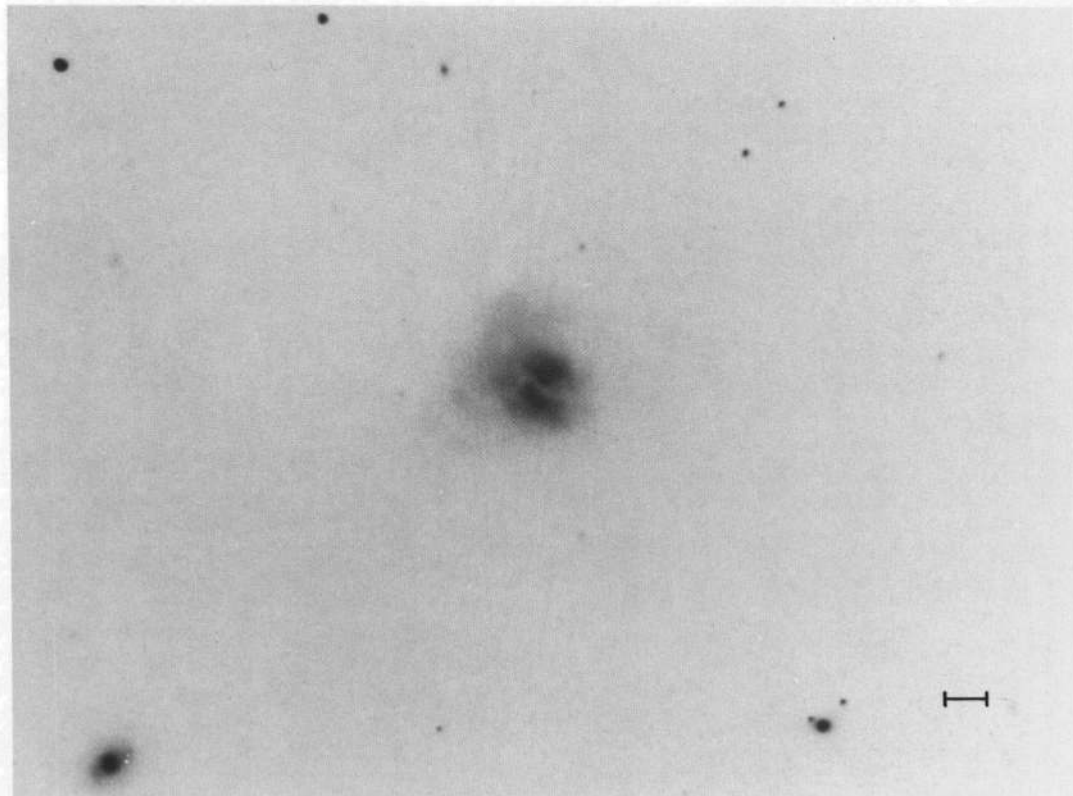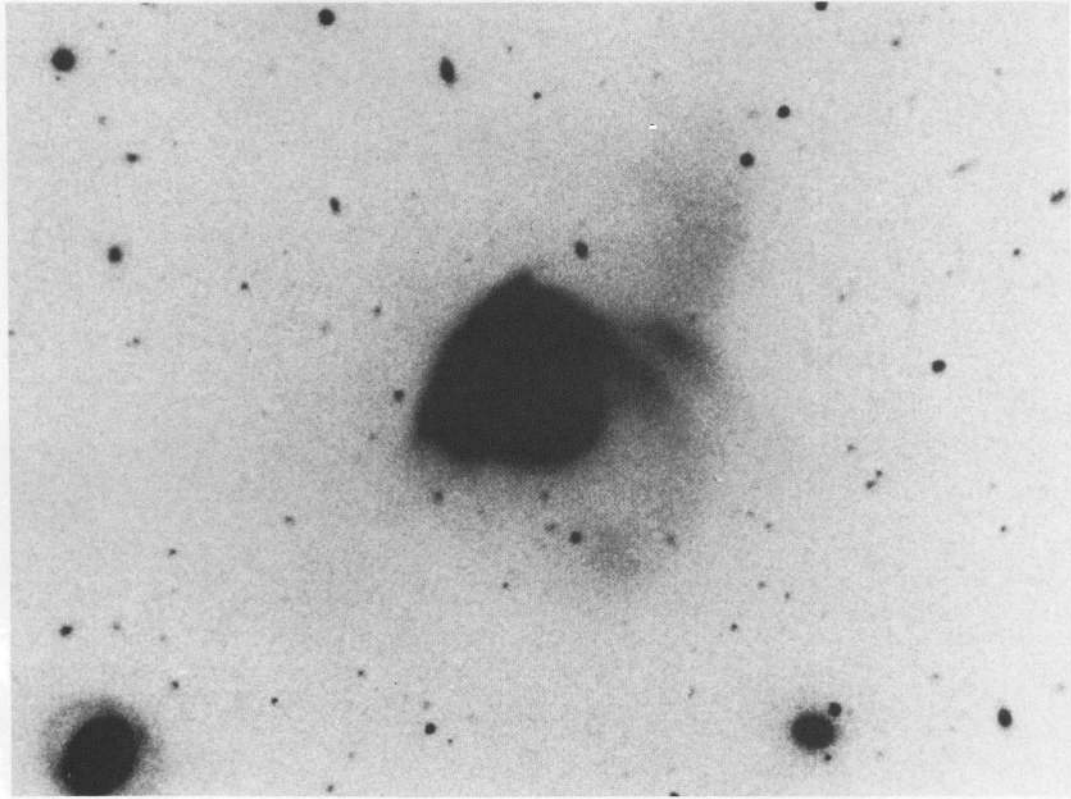
FIG. 10.—*IRAS* 15327 + 2340 = Arp 220

PLATE 18

FIG. 11.—*IRAS* 22491−1808

IRAS 08572+3915

IRAS 05189−2524

Markarian 231

UGC 05101

IRAS 12112+0305

FIG. 1.—Contour maps from CCD images at 6500 Å (Gunn *r*) of the 10 ultraluminous infrared galaxies from the *IRAS* Bright Galaxy Survey. Contour intervals are a factor of 2 apart. The axes are labeled in arcseconds.

76

Markarian 273

IRAS 14348-1447

IRAS 15250+3609

Arp 220

IRAS 22491-1808

FIG. 1.—*Continued*

77
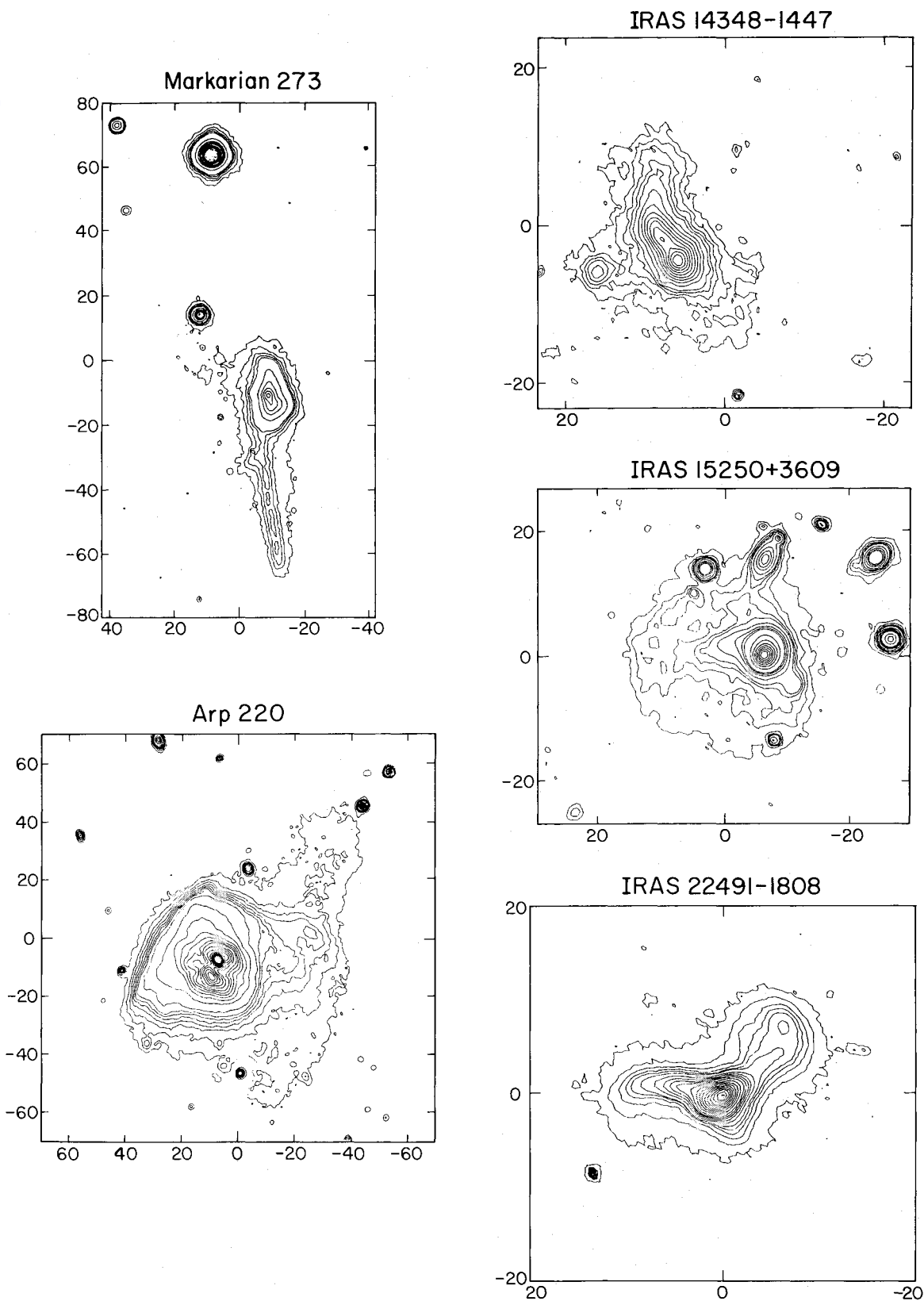
argue that the two counterrotating, "tidal-tails" are a clear signature (Toomre and Toomre 1972) that this object is a merger of two spiral galaxies. A similar image was obtained by Hutchings and Neff (1987) who also suggest that Markarian 231 is a merger system.

d) *Optical Spectra*

Long-slit, optical spectra in both the red and the blue have been obtained for all of the ultraluminous galaxies using the double spectrograph on the Palomar 5 m telescope. Coverage in the blue was 3500–5500 Å at a resolution of 8 Å, and in the red was 5500–7800 Å at a resolution of 12 Å. Seeing was 1″ to 1″.5, and the slit width was 2″. For double nuclei the spectrograph was rotated so that both nuclei were centered in the slit.

The combined red and blue spectra for each object are shown in Figure 12. All of the ultraluminous galaxies are emission-line objects, with the nucleus dominating the emission in every case. There was no evidence of secondary bumps in the collapsed, long-slit data which would be indicative of prominent disk emission.

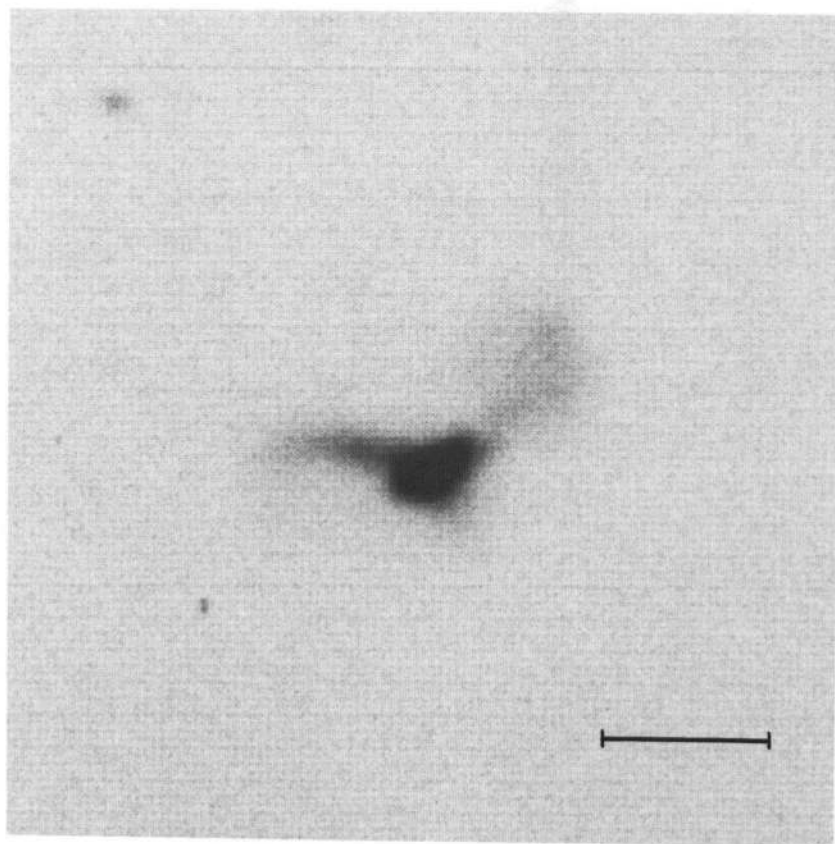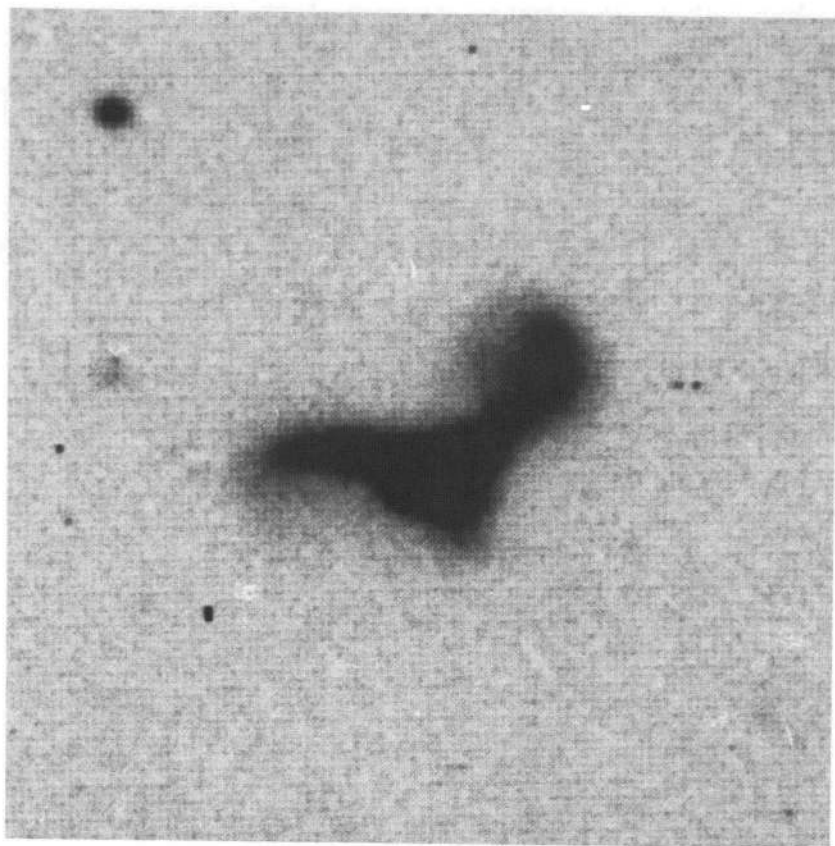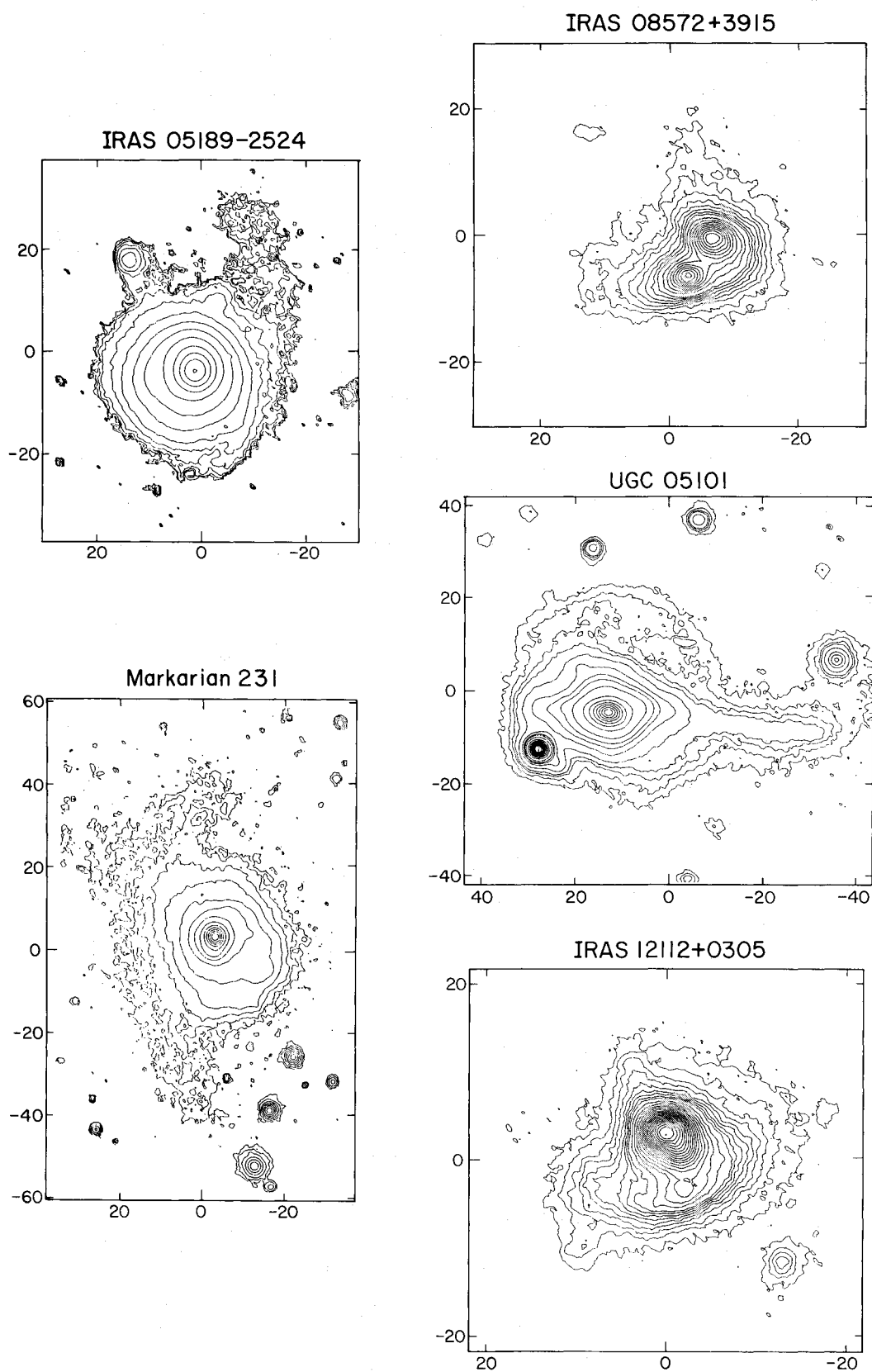Three of the ultraluminous galaxies—Mrk 231, UGC 05101, and *IRAS* 05189−2524—have Hα line widths (full-width at zero intensity, FWZI) greater than 2000 km s^{-1}. Mrk 231 has previously been classified as a Seyfert 1 nucleus (Markarian 1969) on the basis of the extremely broad Hα emission. Based both on the shape of the Hβ line and the relatively broad Hα line, UGC 05101 and *IRAS* 05189−2524 would probably be classified as Seyfert 1.5 and Seyfert 1.8, respectively (see, e.g., Osterbrock 1984).

Six of the remaining seven galaxies have Hα line widths

(FWZI) in the range 1000–2000 km s^{-1}, and would appear to be either Seyfert 2 or low-ionization nuclear emission-line (LINER) galaxies based both on the line width and their relatively large [O III]/Hβ ratios. Mrk 273 has previously been classified as a Seyfert 2 nucleus (Khachikian and Weedman 1974). Heckman *et al.* (1983) were unable to distinguish between classifying Arp 220 as a Seyfert or LINER.

Of the ultraluminous objects *IRAS* 22491−1808 has the smallest observed Hα width (FWZI ≲ 500 km s^{-1}), and the largest observed [O III]/Hβ ratio suggesting that its optical spectrum is dominated by thermal emission from H II regions (French 1980).

e) *Optical and Near-Infrared Photometry*

Photometric images in standard filters (B, g, r, i) were obtained of each galaxy using the CCD camera with reimaging optics on the Palomar 1.5 m telescope. Near-infrared measurements in the J (1.3 μm), H (1.65 μm), K (2.2 μm), and L' (3.7 μm) bands have been made using a 5″ or 10″ diameter beam with the Palomar 5 m telescope. Measurements were also made at N (10.1 μm) with a 4″.6 beam using the 5 m telescope. The observed optical and near-infrared data are tabulated in Table 3. Optical magnitudes for the central 5″ and 10″ regions of each galaxy are listed for comparison with the near-infrared photometry.

f) *CO(1 → 0) Emission*

Previous observations of Arp 220 (Young *et al.* 1984; Sanders and Mirabel 1985) and Mrk 231 (Sanders *et al.* 1987a) have shown these two objects to be extremely luminous in the

TABLE 3
OPTICAL AND NEAR-INFRARED MAGNITUDES

IRAS	B 0.44 μm	g 0.49 μm	r 0.66 μm	i 0.82 μm	J 1.3 μm	H 1.6 μm	K 2.2 μm	L' 3.7 μm	N[a] 10.1 μm	Beam (″)
05189−2524.........	17.03	16.80	16.84	16.81	12.72	11.45	10.22	8.28	4.65	5
	15.90	15.90	15.40	15.20	12.60	11.36	10.16	8.27	...	10
	15.30	14.95	14.61	14.39	...	...	...	...	...	50
08572+3915.........	17.30	16.90	16.70	16.55	15.60	14.65	13.11	9.50	5.45	5
	16.21	15.95	15.42	15.10	15.06	14.24	12.92	9.44	...	10
	14.82	14.42	14.11	13.90	...	...	...	...	...	50
09320+6134.........	16.62	16.42	16.40	16.35	13.16	12.21	11.13	9.79	6.08	5
	15.54	15.52	15.21	15.28	12.72	11.79	10.93	9.77	...	10
	14.90	14.64	14.27	14.08	...	...	...	...	...	50
12112+0305.........	18.60	18.03	17.96	18.23	14.86	13.94	13.25	12.70	7.09	5
	17.73	17.21	17.04	17.06	...	...	...	...	...	10
	16.92	16.05	15.75	15.41	...	...	...	...	...	50
12540+5708.........	13.83	13.81	13.73	13.68	11.35	10.04	8.87	7.16	3.71	5
	13.21	13.63	13.22	13.11	11.28	10.03	8.83	7.05	...	10
	12.90	12.50	12.21	12.03	...	...	...	...	...	50
13428+5608.........	16.91	16.44	15.93	15.82	13.16	12.26	11.57	10.44	6.24	5
	15.80	15.52	15.02	15.26	...	...	...	...	...	10
	14.90	13.98	13.58	13.60	...	...	...	...	...	50
14348−1447.........	18.21	17.93	17.33	17.01	14.98	14.09	13.27	...	>5.97	5
	17.43	17.02	16.61	16.58	...	...	...	...	...	10
	16.72	16.07	15.65	15.34	...	...	...	...	...	50
15250+3690.........	18.05	17.77	17.42	17.44	14.33	13.57	13.05	12.08	6.85	5
	17.21	16.83	16.61	16.72	...	...	...	...	...	10
	16.22	15.64	15.30	15.29	...	...	...	...	...	50
15327+2430.........	16.62	15.56	15.47	15.28	13.09	11.94	11.18	10.15	5.60	5
	15.43	14.61	14.36	14.37	12.31	11.33	10.70	10.02	...	10
	14.00	13.36	13.23	13.16	...	...	...	...	...	50
22491−1808.........	18.20	18.05	17.90	17.87	14.73	14.01	13.55	>12.64	>7.45	5
	17.50	17.10	16.83	16.80	...	...	...	...	...	10
	16.47	16.06	15.82	15.71	...	...	...	...	...	50
unc(±)	(0.05)	(0.05)	(0.05)	(0.05)	(0.07)	(0.07)	(0.07)	(0.10)	(0.20)	

[a] 10 μm beamsize was 4″.6.
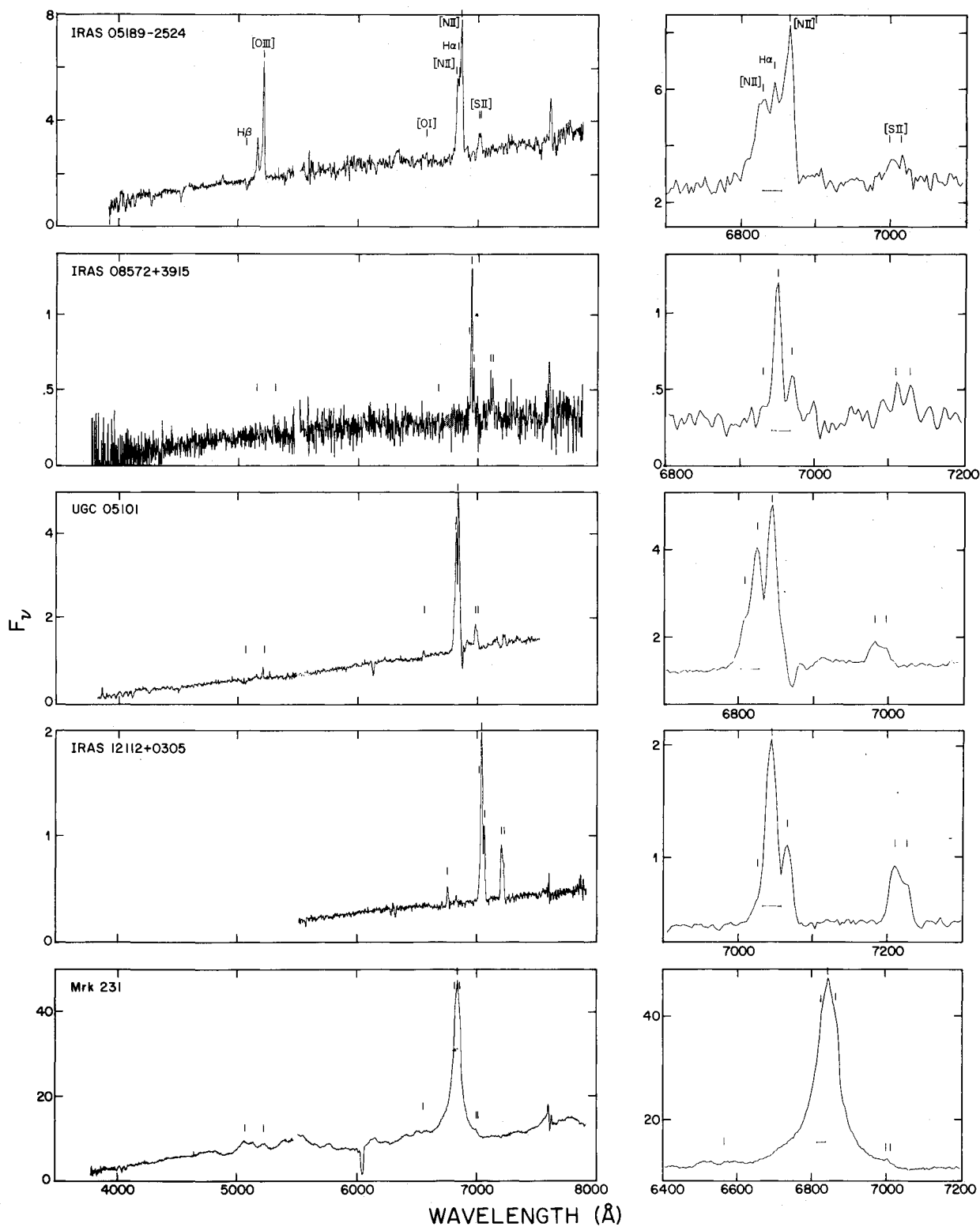
FIG. 12.—Optical spectra ($\lambda\lambda$ 3800–7500) of ultraluminous infrared galaxies obtained with the double spectrograph on the Palomar 5 m telescope. Integration times varied between 10 and 25 minutes. An expanded plot in the wavelength range of Hα + [N II] is shown on the right. The horizontal line corresponds to 1000 km s^{-1}. Vertical scale is energy flux in flux units per unit frequency interval.
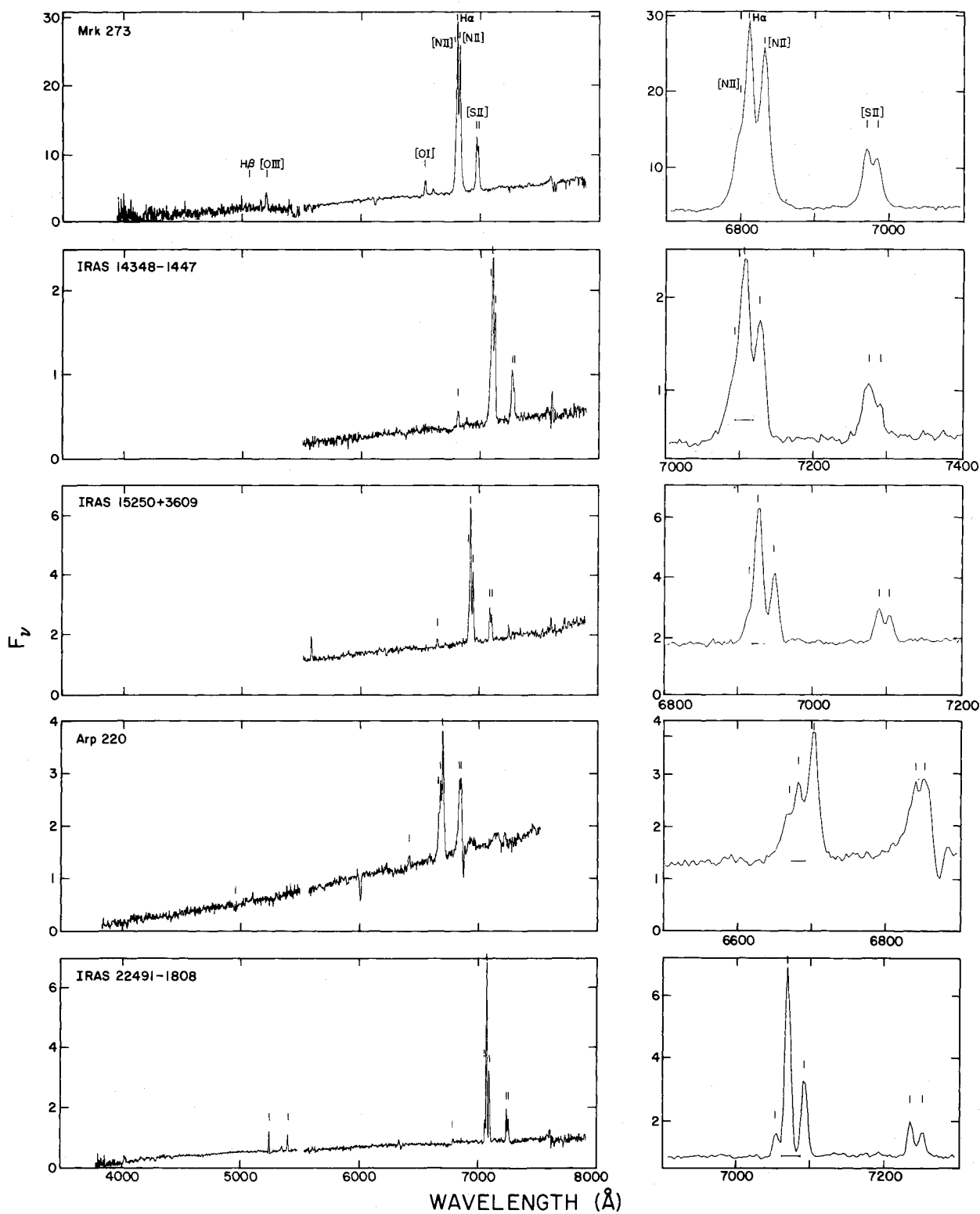
FIG. 12.—Continued

TABLE 4

CO(1 → 0) EMISSION

IRAS	I_{CO}[a] (K km s^{-1})	log L_{CO} (K km s^{-1} pc^2)
05189−2524.........	2.6	9.63
12112+0305.........	1.5	9.85
12540+5708.........	1.6	9.42
13428+5608.........	2.3	9.48
14348−1447.........	1.7	10.03
15327+2340.........	11.5	9.34
22491−1808.........	0.9	9.66
unc(σ)	±10%	±0.04

[a] NRAO 12 m telescope (Sanders, Scoville, and Soifer 1987).

CO(1 → 0) emission line, indicating that they are rich in molecular gas. A recently completed CO(1 → 0) survey of galaxies in the *IRAS* Bright Galaxy Sample (Sanders, Scoville, and Soifer 1987) includes five additional ultraluminous galaxies, and all five rank among the most luminous CO sources discovered to date. Table 4 gives the CO luminosities for all of the ultraluminous galaxies that have been detected in the CO(1 → 0) emission line.

III. PROPERTIES OF ULTRALUMINOUS IRAS GALAXIES

a) Morphology

The contour maps (Fig. 1) and optical images (Figs. 2–11) suggest that all of the ultraluminous objects are strongly interacting galaxies. The majority are best described as ongoing mergers. According to Toomre and Toomre (1972), principal pieces of evidence for a recent merger are the presence of tidal tails, and of multiple nuclei or disks. Seven of the objects exhibit major tidal tails *plus* main bodies that appear to be overlapping or perhaps not even separable, similar in appearance to the sample of ongoing mergers described by Toomre (1977). Four of the seven—*IRAS* 05189−2524, Mrk 231, Arp 220, and *IRAS* 22491−1808—appear to be nearly completed mergers based on the detection of two tidal tails which indicate the presence of two strongly interacting spiral disks, but only a

single identifiable nucleus. Also the large size and symmetry of the tails indicates that, in each of these objects, both spiral galaxies were of roughly equal mass (Toomre and Toomre 1972). The remaining three—*IRAS* 08572+3915, *IRAS* 12112+0305, and *IRAS* 14348−1447—each show two nuclei which are separated by less than 5 kpc. The deep optical images of these three objects also indicate that they are composed of two galaxies of roughly equal size.

Of the three objects that do not show evidence for an ongoing *merger*, two exhibit prominent rings, and have nearby companions. Such rings are thought to result from near face-on collisions between spiral disks (Lynds and Toomre 1976), and this is assumed to be the case in UGC 05101 and *IRAS* 15250+3609. The remaining object, Mrk 273, shows only a single long tail which is most likely the result of a collision of a large spiral galaxy and a galaxy of much smaller mass (Toomre and Toomre 1972). A strong candidate for the collision partner is the galaxy with similar redshift which is ∼40″ north of Mrk 273 along the line defined by the tail.

b) Optical Emission Lines

To characterize the dominant energy source producing the line emissions in the ultraluminous galaxies we have followed the work of Veilleux and Osterbrock (1987), using four line ratios—([O III] λ5007)/(Hβ λ4861), ([S II] λ6716+λ6731)/(Hα λ6563), ([N II] λ6583)/(Hα λ6563), ([O I] λ6300)/(Hα λ6563)—to provide maximum discrimination between thermal and nonthermal sources of ionizing radiation. The measured and dereddened line ratios derived assuming the intrinsic Hα/Hβ ratio is 2.9, and the derived reddenings, $E(B−V)$, are listed in Table 5. Figure 13 plots the four line ratios for all of the sample galaxies except the obvious Seyfert 1 galaxy Mrk 231. All but one of the nine galaxies plotted in Figure 13 fall clearly within the line ratio region characteristic of active nuclei rather than the region occupied by thermally excited objects.

As a class, the emission-line spectra of the ultraluminous infrared galaxies differ dramatically from the spectra of lower luminosity *IRAS* galaxies. The vast majority of the bright infrared galaxies surveyed by Sanders *et al.* (1987c), as well as the infrared galaxies in the *IRAS* minisurvey studied by Elston, Cornell, and Lebofsky (1985), and by Lawrence *et al.* (1986)

TABLE 5

MEASURED AND CORRECTED OPTICAL EMISSION-LINE RATIOS

| IRAS	log [O III]/H$_\beta$	log [N II]/H$_\alpha$	log [S II]/H$_\alpha$	log [O I]/H$_\alpha$	log (H$_\alpha$/H$_\beta$)	$E(B−V)$
05189−2524.........	1.56	0.21	−0.35	−0.83	1.24	1.62
	1.47	0.21	−0.40	−0.63	0.49	
08572+3915.........	0.63	−0.39	−0.37	−0.99	1.45	2.06
	0.53	−0.39	−0.44	−0.73	0.49	
09320+6134.........	0.67	0.07	−0.41	−1.23	0.92	0.93
	0.62	0.07	−0.44	−1.04	0.49	
12112+0305.........	0.40	−0.41	−0.39	−1.12	1.48	2.12
	0.37	−0.41	−0.43	−1.01	0.49	
13428+5608.........	0.57	−0.06	−0.30	−1.12	0.75	0.56
	0.55	−0.06	−0.33	−1.01	0.49	
14348−1447.........	0.48	−0.25	−0.39	−1.26	1.35	1.83
	0.43	−0.25	−0.42	−1.09	0.49	
15250+3609.........	0.79	−0.41	−0.29	−1.14	1.21	1.43
	0.73	−0.41	−0.33	−0.96	0.49	
15327+2340.........	1.03	0.11	−0.14	−0.85	1.55	2.30
	0.92	0.11	−0.17	−0.61	0.49	
22491−1808.........	−0.01	−0.34	−0.49	−1.62	0.90	0.89
	−0.05	−0.35	−0.52	−1.51	0.49	
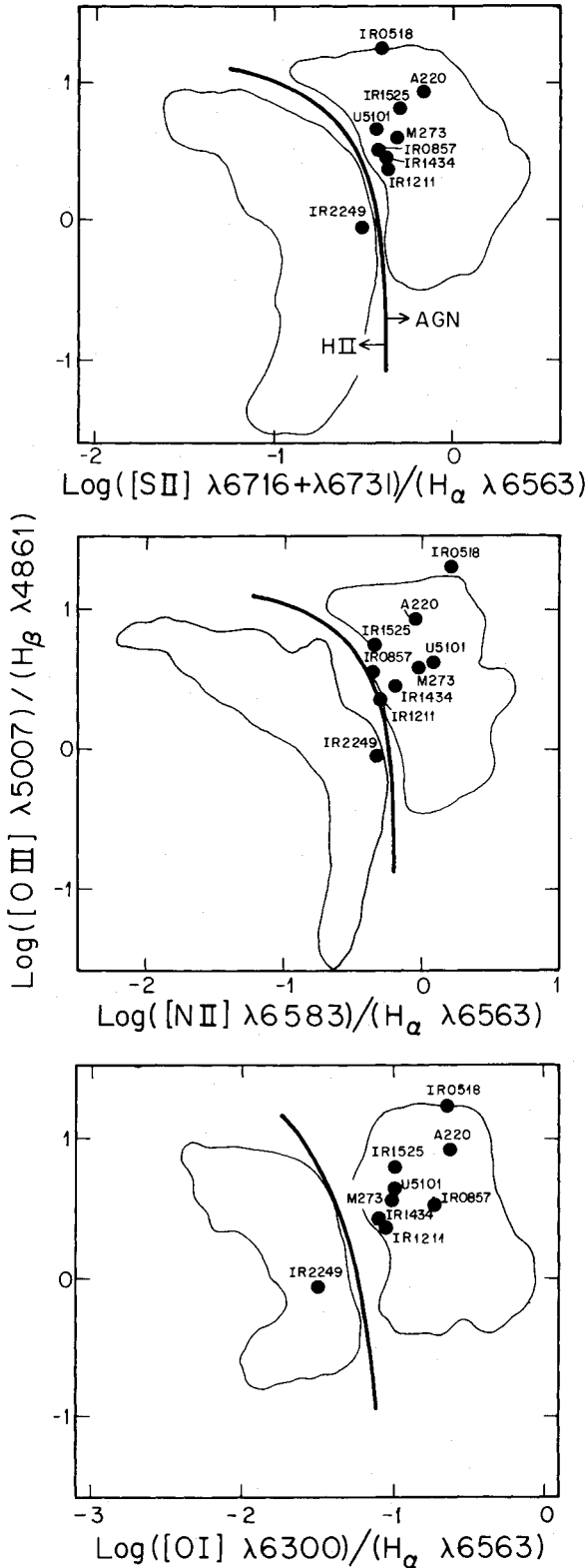
FIG. 13.—Reddening-corrected optical emission-line intensity ratios for ultraluminous infrared galaxies: (*top*) [O III] $\lambda5007$/Hβ vs. [S II] ($\lambda6716 + \lambda6731$)/H$\alpha$; (*middle*) [O III] $\lambda5007$/Hβ vs. [N II] $\lambda6583$/Hα; (*bottom*) [O III] $\lambda5007$/Hβ vs. [O I] $\lambda6300$/Hα. In each panel the thick solid curve divides AGNs from H II region–like galaxies, while the outlined regions represent the locus of AGN and H II region–like galaxy spectra as summarized in Veilleux and Osterbrock (1987).

have very narrow optical emission lines ($\lesssim300$ km s^{-1}) and line intensity ratios characteristic of emission from H II regions.

c) Near-Infrared Colors

Figure 14 plots $J - H$ versus $H - K$ for each of the ultraluminous galaxies and compares their colors with those of normal spirals, *IRAS* minisurvey galaxies, the nearby starburst galaxies M82 and NGC 253, and several quasars. The rest frame colors of the ultraluminous infrared galaxies were determined by making only the K-corrections to the infrared magnitudes listed in Table 3 using the expression for the K-correction $f_\nu(\text{emit}) = f_\nu(\text{obs}) \times K(z)$ where $K(z) = (1 + z)^{1+\alpha}$ (see Neugebauer *et al.* 1985), where the power-law slope α was determined for each band by a linear interpolation through the observed data points.

The $J - H$ and $H - K$ colors for the ultraluminous galaxies cover a significantly larger range than the colors of either normal spirals or the lower luminosity *IRAS* galaxies, and there is almost no overlap with either of these lower luminosity classes. Several of the ultraluminous infrared galaxies have colors which could be accounted for simply by dereddening M82, which is typical of intermediate luminosity starburst galaxies; thus, on the basis of infrared colors alone, a starburst cannot be ruled out as the luminosity source in these galaxies. However, even if reddening is taken into account [for example, by using the $E(B - V)$ values listed in Table 5] the majority of the ultraluminous galaxies still appear to be completely unlike the lower luminosity infrared objects; their infrared colors are more similar to those of active nuclei and quasars.

d) 10 μm Compactness

Knowledge of the distribution of gas and far-infrared flux in the ultraluminous infrared objects allows an obvious critical test for discriminating among the various models for producing the far-infrared luminosity. At present, high-resolution far-infrared "maps" do not exist for any of the ultraluminous galaxies, except for the drift scan deconvolution of the 100 μm emission from Arp 220 (Joy *et al.* 1986), that indicates a diameter smaller than 7" for the far-infrared source. Near-infrared maps of 10 μm and 20 μm emission at 2" resolution (Becklin and Wynn-Williams 1987) show a source less than or equal to 2" diameter containing most of the emission in Arp 220. For Mrk 231, Matthews *et al.* (1987) find a dominant point source ($\leq 0''.5$ diameter) at 10 μm from an analysis of slit scans made with the Palomar 5 m telescope. Both of these results favor an AGN model for the central power source, since a star-formation origin would lead to a more extended emission region.

For the remaining objects it has only been possible to estimate the degree of central concentration of the far-infrared emission by obtaining 10 μm observations with a 4''.6 diameter beam on the Palomar 5 m telescope for comparison with the *IRAS* 12 μm flux. If the true 10 μm/12 μm flux density ratio is ~ 0.8, as indicated from an extrapolation of the *IRAS* data, the small beam contains more than 80% of the total 10 μm flux for all of the ultraluminous galaxies. At similar redshifts, normal molecular gas-rich spirals like M101 or IC 342 would have less than ~ 30% of their 10 μm flux in a 4''.6 beam, thus all of the ultraluminous infrared objects show an abnormal nuclear concentration of 10 μm emission. However, the 4''.6 beam which corresponds to ~ 4.5 kpc at a redshift of 0.05 is still too large to provide a very useful constraint on the "point-source" contri-
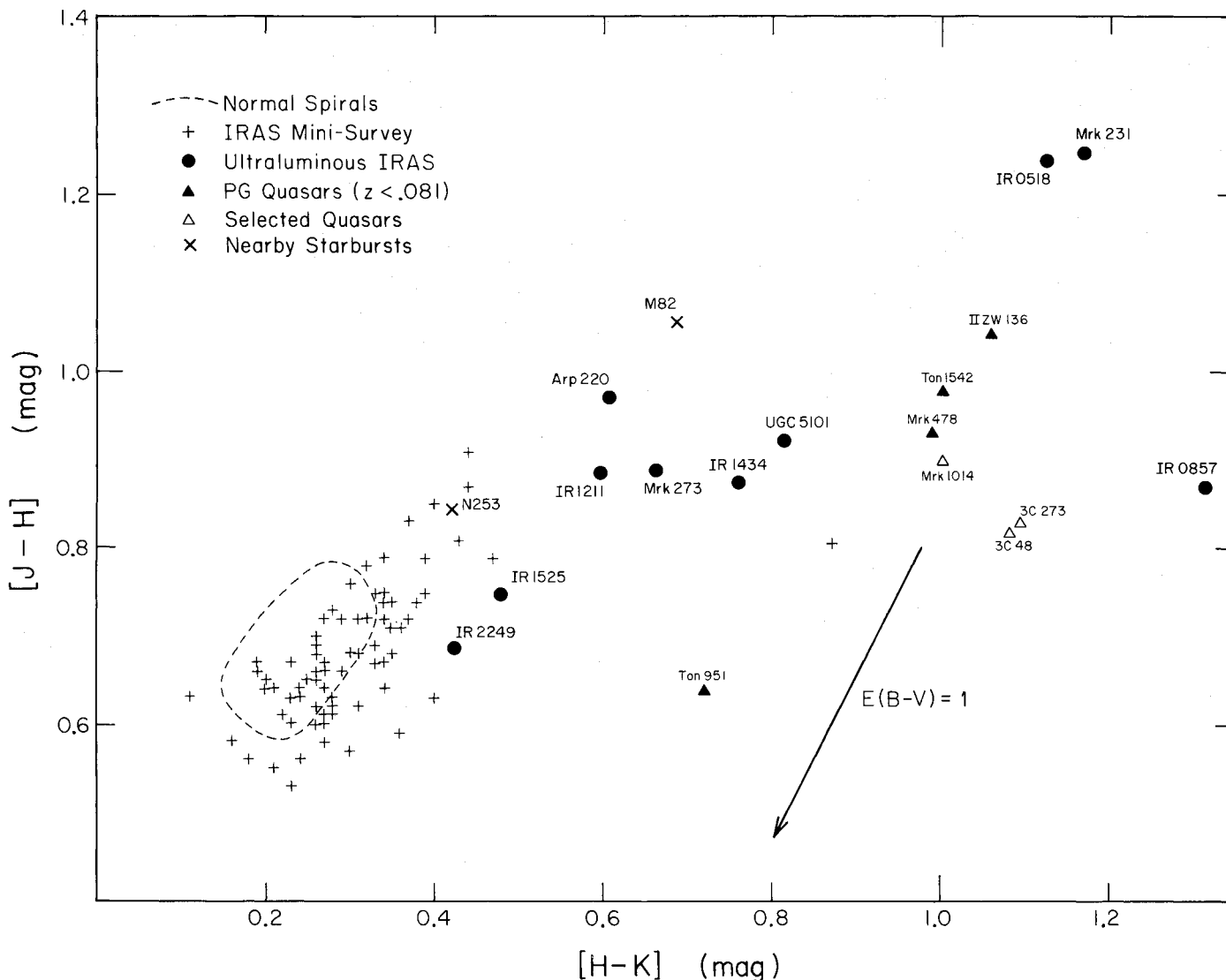
FIG. 14.—Comparison of near-infrared colors of ultraluminous infrared galaxies with normal spirals, less luminous infrared galaxies, and quasars. Dashed area for normal spirals is taken from Aaronson (1977) and the *IRAS* minisurvey data are from Carico *et al.* (1986). Data for the nearby starburst galaxies M82 and NGC 253 and the Palomar-Green quasars are from Neugebauer *et al.* (1986).

bution to the 10 μm emission (presumably of nonthermal origin).

e) *Energy Distribution*

The *IRAS* data have been combined with the ground-based optical and near-infrared photometry to determine the energy spectrum between 0.44 and 100 μm for all of the ultraluminous galaxies as shown in Figure 15. The dominance of the far-infrared emission ($\lambda \geq 40$ μm) in the total energy budget can easily be seen: the fraction of total luminosity contributed by emission at $\lambda \geq 40$ μm ranges from more than 95% for *IRAS* 12112+0305 to ~50% in Mrk 231.

The energy distributions in Figure 15 are displayed approximately in order of increasing $f_\nu(60\ \mu\text{m})/f_\nu(100\ \mu\text{m})$ ratio of flux densities (from top to bottom). The 60 μm and 100 μm *IRAS* data points have been fitted with a single-temperature dust emission model ($\epsilon \propto \lambda^{-1}$). There is an obvious trend of increasing 12 μm and 25 μm emission with increasing $f_\nu(60\ \mu\text{m})/f_\nu(100\ \mu\text{m})$ color temperature, possibly due to a separate component

of hotter dust associated with a Seyfert nucleus (see Miley, Neugebauer, and Soifer 1985). There is also a trend of increasing 1–5 μm flux with warmer far-infrared color temperature. This may still represent thermal emission from high-temperature dust relatively close to a luminous nonthermal nuclear source, or it could also be due to an increasing non-thermal component directly associated with the region emitting the broad optical emission lines.

f) *Molecular Gas*

H_2 masses have been computed from the CO luminosities listed in Table 4 using the relation $N(H_2) = 3.6 \times 10^{20} \int T(\text{CO})dv$ [cm^{-2}(K km s^{-1})$^{-1}$], found for molecular clouds in the Milky Way (Sanders, Solomon, and Scoville 1984). The mass estimates, given in Table 6, imply that the ultraluminous infrared galaxies have 3–20 times the H_2 content of the Milky Way. The relatively large H_2 masses found for the ultraluminous galaxies are not unexpected given the results of previous CO observations of *IRAS* bright gal-
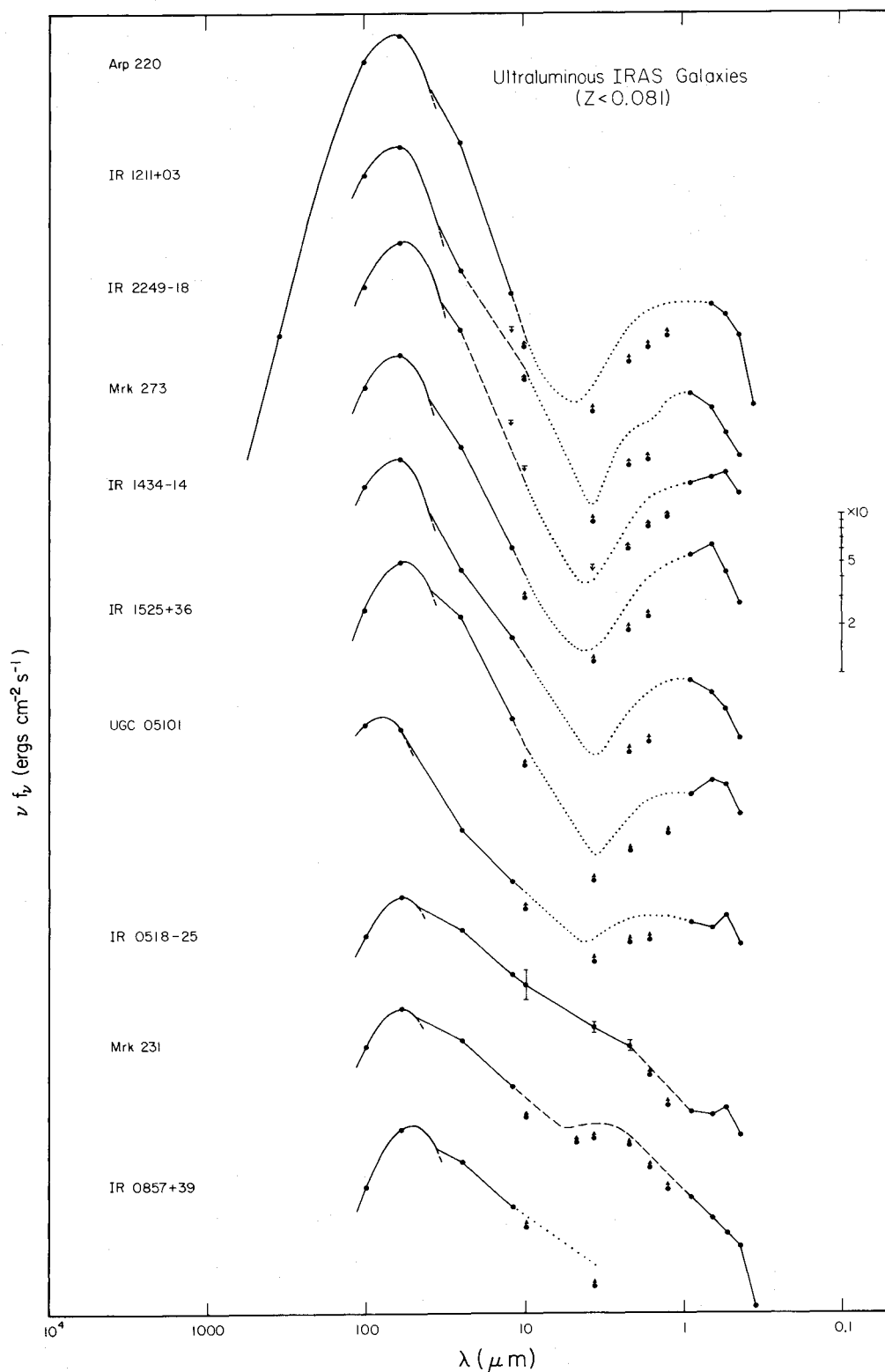
FIG. 15.—Spectral energy distributions from 0.33 to 100 μm for ultraluminous infrared galaxies in the *IRAS* Bright Galaxy Survey. Data from 0.44 to 100 μm are from this work. Additional data for Arp 220 at 350 μm and 760 μm are from Emerson *et al.* (1984). The 1–10 μm data points are 5″ or 10″ aperture measurements. The shape of the energy distribution of the entire galaxy between 1 and 10 μm (*dotted line*) was estimated from these small beam measurements and the measured magnitude growth curve at *I*(0.88 μm).

TABLE 6

MOLECULAR GAS AND DUST

IRAS	$M(H_2)$ $(10^{10} M_\odot)$	$L_{fir}/M(H_2)^a$ $(L_\odot M_\odot^{-1})$	T_D (K)	$150M_D$ $(10^{10} M_\odot)$
05189−2524........	2.4	35	53	0.3
08572+3915........	...	...	66	0.2
09320+6134........	...	...	38	1.5
12112+0305........	4.2	38	44	1.6
12540+5708........	1.5	135	50	1.0
13428+5608........	1.7	66	50	0.6
14348−1447........	6.1	27	46	1.4
15250+3609........	...	...	55	0.2
15327+2340........	1.4	96	45	1.1
22491−1808........	2.7	43	53	0.4
Mean ± σ	2.8 ± 1.5	63 ± 32		0.8 ± 0.5

^{a} $L_{fir} = L(40–400 \mu m)$.

axies at lower luminosity. A recent survey of CO(1 → 0) emission from galaxies in the *IRAS* Bright Galaxy Sample with infrared luminosities 10^{11}–10^{12} $L_\odot$ (Sanders *et al.* 1986) has shown that all of these galaxies are rich in molecular gas, having total masses of H_2 ranging from 10^9 to 3×10^{10} $M_\odot$. The ultraluminous infrared galaxies all have H_2 masses near the upper end of this range.

In addition to the total molecular gas masses calculated from the single-beam CO data there is, in Arp 220, also a direct measurement of the degree of central concentration of the CO emission from interferometer observations (Scoville *et al.* 1986), which show that more than 70% of the CO emission,

corresponding to $\sim 10^{10}$ $M_\odot$ of H_2, comes from a nuclear source smaller than 6″ in diameter (1.5 kpc).

As a check on the H_2 masses derived from CO, dust masses were also computed by fitting the 60 μm and 100 μm *IRAS* fluxes with a single-temperature dust model and dust emissivity, $\epsilon \propto \lambda^{-1}$. If the gas-to-dust ratio is 150, the mean gas masses computed from the two different methods are in relatively good agreement. The seven galaxies detected in CO have a mean ratio, $M(H_2)/150M_D = 3.4$ with a sample dispersion of ±1.5. Considering the uncertainties in the dust and gas mass calculations this is excellent agreement.

The second column in Table 6 lists the $L_{fir}/M(H_2)$ ratio which provides a measure of the luminosity per unit mass of molecular gas. The mean $L_{fir}/M(H_2)$ ratio for the seven galaxies detected in CO is 63 ± 32 $L_\odot M_\odot^{-1}$, as compared with 3–7 $L_\odot M_\odot^{-1}$ for normal spiral galaxies like the Milky Way and M101, and 12–25 $L_\odot M_\odot^{-1}$ for starburst galaxies like M82 and NGC 253 (see Fig. 16). The mean $L_{fir}/M(H_2)$ ratio for the ultraluminous galaxies also exceeds the largest value observed in molecular clouds in our own Galaxy. The maximum $L_{fir}/M(H_2)$ ratio observed in Galactic giant molecular clouds (GMC) is ~ 30 $L_\odot M_\odot^{-1}$ (Scoville and Good 1987; Solomon *et al.* 1987), with such large values being extremely rare and confined to the most massive and active star-forming cloud cores such as M17 and W51.

g) Summary of Properties and Comparison with Lower Luminosity IRAS Galaxies

Table 7 summarizes the global properties of ultraluminous infrared galaxies and compares them with lower luminosity
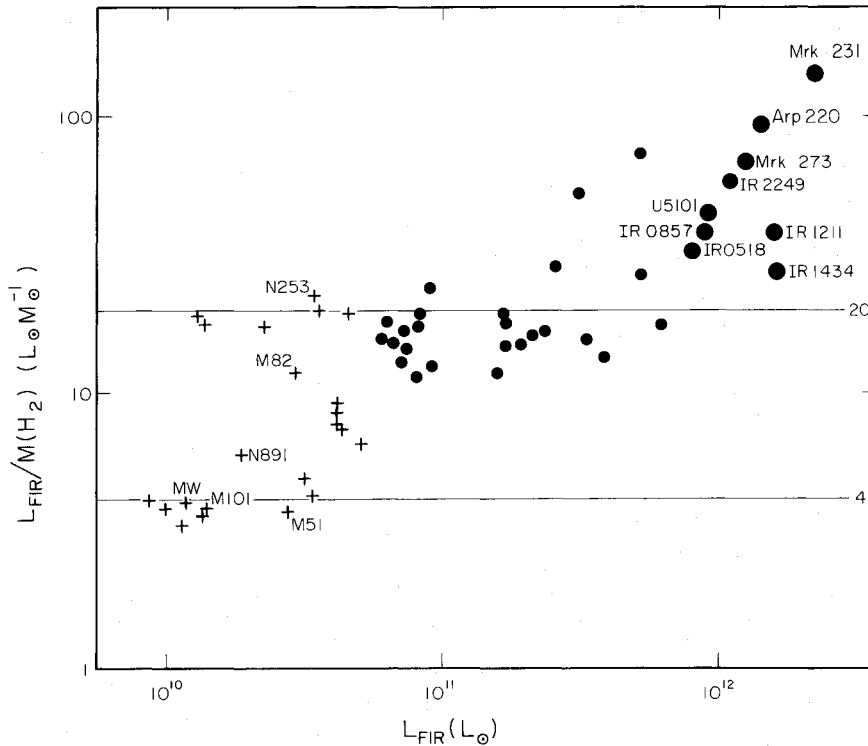

FIG. 16.—Ratio of total *IRAS* far-infrared luminosity and total H_2 mass in molecular clouds vs. L_{fir} for bright *IRAS* galaxies. The ultraluminous infrared galaxies are represented by large circles. Small circles represent "high-luminosity" *IRAS* galaxies which are an unbiased sample of all galaxies with $L_{fir} \gtrsim 7 \times 10^{10}$ $L_\odot$ (Sanders *et al.* 1986). Plus symbols represent CO observations of lower luminosity bright *IRAS* galaxies with known and unknown selection bias—primarily local late-type spirals and low-redshift bright *IRAS* galaxies from the early *IRAS* circulars. The straight solid lines represent an $L_{fir}/M(H_2)$ value of $4 L_\odot M_\odot^{-1}$, typical of the mean value found for molecular gas rich spirals, and an $L_{fir}/M(H_2)$ value of 20 $L_\odot M_\odot^{-1}$ characteristic of the nearby starburst galaxies M82 and NGC 253.

TABLE 7

IRAS Galaxy Properties vs. Increasing Infrared Luminosity[a]

Property		Moderate Luminosity (10^{10}–10^{11} $L_\odot$)	High Luminosity (10^{11}–10^{12} $L_\odot$)	Ultraluminous ($\geq 10^{12}$ $L_\odot$)
Number of objects[b]		80	80	10
Morphology	Strongly interacting	10	40	100
(percentage)	close pair	15	30	0
	isolated	75	30	0
Ionizing source	AGN	10	30	90
(percentage)	H ɪɪ	90	70	10
$\nu f_\nu(80)/\nu f_\nu(B)$ .... (median)		1	5	25
$L_{\rm fir}/M({\rm H}_2)[L_\odot\,M_\odot^{-1}]$ .... (mean)		4	15	63

[a] Infrared luminosity = $L(8$–$1000\ \mu{\rm m})$. Data for moderate luminosity and high-luminosity galaxies are from Sanders *et al.* (1986, 1987*b*).

[b] Galaxies in the *IRAS* Bright Galaxy Survey (Soifer *et al.* 1986, 1987).

IRAS galaxies. All of the ultraluminous galaxies are strongly interacting systems. Nine out of 10 show optical emission-line ratios implying dominant nonthermal ionizing sources and are extremely rich in molecular gas. The data presented in Table 7 show that the ultraluminous infrared galaxies represent the culmination of a trend toward an increasing percentage of strongly interacting systems with increasing infrared luminosity. Below $\sim 10^{11}$ $L_\odot$ the vast majority of infrared galaxies appear to be single noninteracting spirals whose infrared luminosity can be accounted for largely by star formation. As the infrared luminosity increases above 10^{11} $L_\odot$ there is both a dramatic increase in the frequency of strongly interacting systems, and evidence from the optical spectra of a dominant, nonthermal active nucleus.

IV. ORIGIN AND EVOLUTION OF ULTRALUMINOUS INFRARED GALAXIES

The study of the *IRAS* Bright Galaxy Survey has demonstrated the existence of a class of ultraluminous infrared galaxies which are more numerous, and bolometrically as luminous as optically selected quasars in the local universe ($z \lesssim 0.1$). The dominant nonthermal ionization as probed by the optical emission lines, the extreme near-infrared colors, and the large $L_{\rm fir}/M({\rm H}_2)$ ratios strongly suggests that the dominant luminosity source in the ultraluminous infrared galaxies is a nonthermal AGN, and when coupled with their quasar-like luminosity, is sufficient evidence to argue that the majority, if not all of these objects, are in fact dust-enshrouded quasars. This interpretation is further supported by the more extensive data for Arp 220 and Mrk 231—the extremely small 10 μm and 20 μm sizes (§ III*d*), plus the broad Brα line emission in Arp 220 reported recently by Depoy (1987).

The optical images of the ultraluminous infrared objects suggest strongly that the trigger for producing these quasar-like luminosities is galaxy collisions. Below we outline a simple idealized model for the formation of ultraluminous infrared galaxies which involves the merger of two molecular gas-rich spirals. Dust is assumed to play an important role in determining the shape of the energy distribution of the interacting system, and observations are presented to illustrate the proposed evolution of the energy distribution from one of infrared

excess to one dominated by ultraviolet and X-ray emission as the quasar nucleus emerges from its dust shroud.

a) Model

The model assumes a merger of two late-type spiral galaxies as the optimum interaction for producing maximum nuclear luminosity. A merger ensures maximum disk overlap, hence maximum collision rates for molecular clouds. The choice of late-type spirals increases the likelihood of starting out with a large mass of gas, plus a large fraction of this gas at small galactocentric radii (see review by Young 1986).

Once the inner disks of the two galaxies overlap sufficiently, molecular cloud collisions will occur frequently. Assuming a cloud mean free path of 1–2 kpc, typical of the inner disks of late-type spirals (Sanders, Scoville, and Solomon 1985), and reasonable collision velocities of >50 km s^{-1} the time scale for cloud collisions will be on the order of 10^7 yr. At even higher relative velocity such collisions may generate substantial infrared luminosity for short periods, less than $\sim 10^6$ yr (Harwit *et al.* 1987). These collisions should dissipate orbital angular momentum, particularly if the two galaxies have substantial counterrotation. The net cancellation of cloud orbital angular momentum should result in decreased orbit radii and contribute to a funneling of gas into the merger nucleus. Both the concentration of molecular clouds to the merger nucleus and an increased efficiency of star formation due to cloud-cloud collisions (Scoville, Sanders, and Clemens 1986) will result in the appearance of a nuclear "starburst" *before* the merger of the two nuclei. The total time between the beginning of the starburst until its peak should be on the order of 10^8 yr corresponding to the time from the first significant interpenetration of the molecular disks at a nuclear separation of ~ 10 kpc, until the formation of a merger nucleus.

Once the two nuclei have merged, the concentration of molecular gas would presumably be similar to the observed distribution of molecular gas in Arp 220 (Scoville *et al.* 1986), where more than 70% of the total CO emission, corresponding to more than $\sim 10^{10}$ $M_\odot$, is confined to a galactocentric radius smaller than 1 kpc. Self-gravity may play a critical role in the subsequent evolution of the nuclear gas distribution and in the possible feeding of an AGN. The likely formation of a self-gravitating disk, with its inherent instabilities, may provide an

important mechanism for further dissipation of angular momentum and more efficient fueling of the central AGN. The "critical density" required for the onset of gravitational instability in the gas is given by the expression

$$\sigma = \frac{v\kappa}{3.36G} \qquad (1)$$

Toomre (1964), where σ is the gas surface density, v is the one-dimensional velocity dispersion, κ is the epicyclic frequency, and G is the gravitational constant. Assuming a velocity dispersion of 200 km s^{-1}, and a value for κ as large as 300 km s^{-1} kpc^{-1}, the observed average gas surface density over the inner disk of radius 1 kpc in Arp 220 is a factor of 5 larger than the critical surface density.

At the stage represented by the ultraluminous infrared galaxies like Arp 220, it seems reasonable to assume, as our observations indicate, that an AGN contributes significantly, perhaps dominantly to the observed total far-infrared luminosity. The starburst, which was initiated by cloud-cloud collisions, should actually begin to subside, possibly even before this stage. If a massive black hole previously existed in one or both galactic nuclei (Filipenko and Sargent 1985), its accretion disk should experience its maximum accretion rate fueled by the dense interstellar medium enveloping it. If such black holes do not preexist, perhaps the time scale for generating them through a nuclear starburst is sufficiently short that such a process can occur during the merger (e.g., Weedman 1983).

Although we have considered the optimum case of a merger involving two gas-rich spirals, the above model applies to all galaxy collisions in which molecular clouds are the dominant gas constituent. Penetrating collisions in which only one galaxy is gas rich—for example, a collision between an elliptical and spiral—would be expected to produce a smaller increase in total luminosity due to a reduced cloud collision rate and little loss of cloud orbital angular momentum. Likewise, collisions where the inner disks do not interpenetrate should show only a modest increase in luminosity unless some additional mechanism can be found to funnel outer disk gas from one system into the nucleus of the other.

b) Evolution of the Energy Distribution

At the evolutionary stage corresponding to the ultraluminous infrared galaxies, the combined forces of radiation pressure, supernova explosions, stellar winds, etc., should easily be able to disrupt the surrounding gas and push away enough material to open up a hole along a line of sight to the AGN. For example, the rate of momentum transfer to the molecular gas from the AGN luminosity alone, given by

$$\dot{p} = \frac{L_* \tau_R}{c} , \qquad (2)$$

where L_* is the AGN luminosity (assumed to be $10^{12} L_\odot$), and τ_R, the optical depth (assumed to be unity), is sufficient to accelerate $10^{10} M_\odot$ to velocities greater than 100 km s^{-1} in a few times 10^7 yr. Once the dust shroud no longer absorbs all of the luminosity of the AGN there should be a marked change in the spectral energy distribution—a shifting of the far-infrared excess first to shorter infrared wavelengths as the inner regions become visible, then to the optical and UV. We believe this first stage of disrupting the surrounding cloud is the case, as stated earlier, in galaxies like Mrk 231. Once the line of sight to the AGN is relatively unobscured, the energy distribution should

show the UV excess normally associated with the optical quasars. At first, there should not be much change in the total luminosity as the AGN will most likely still have a substantial gas supply from material in and near the flattened accretion disk. The far-infrared color temperature should increase as one sees into the hotter dust closer to the quasar. Finally, once the bulk of the dust and gas has been swept clean of the inner regions the infrared should become insignificant in the total energy budget, and there should be a shifting of the far-infrared luminosity totally to the optical, UV, and X-ray.

Figure 17 demonstrates that the progressive evolution of the energy distribution described above can already be seen in comparing the data for the ultraluminous infrared galaxies with data that have recently become available for previously cataloged quasars. Considering just the sample of ultraluminous infrared galaxies and the small number of local optical quasars there would still be a significant gap in the apparent progression of energy distributions from extreme infrared excess to one of no infrared excess plus a dominant ultraviolet bump. However, the discovery of several more distant (and presumably rarer) optical quasars with substantial infrared excess, as illustrated by the energy distributions for 3C 48 and Mrk 1014, strengthen the case for an orderly progression from ultraluminous infrared galaxy to optical quasar. Objects like 3C 48 and Mrk 1014 have dust temperatures that are sufficiently large that the bulk of their infrared luminosity emerges shortward of the 60 μm band. Searches of the IRAS data base with criteria emphasizing warmer objects appear to have selected such objects with reasonable frequency (see, e.g., deGrijp, Miley, and Lub 1987); in fact, the infrared-loud quasars IRAS 13349 + 2438 (Beichman et al. 1986) and IRAS 00275 − 2859 (Vader and Simon 1987) may also be such examples.

V. DISCUSSION

In the preceding section, we showed that all ultraluminous infrared galaxies apparently develop into quasars. Is the converse also true: do all quasars develop from ultraluminous infrared galaxies? Two lines of evidence suggest that a substantial fraction, if not most quasars form in this way: ultraluminous infrared galaxies and quasars have similar space densities (Soifer et al. 1986); several detailed studies of quasar environments show evidence for recent mergers or interactions with the quasar host galaxies and also indicate that these host galaxies are also fairly gas-rich. This evidence is discussed below.

a) Comparison of Properties of Optical Quasars and Ultraluminous Infrared Galaxies

Perhaps the most surprising and important evidence that ultraluminous infrared galaxies may play a dominant role in the formation of quasars comes from a comparison of their local space densities. The Palomar-Green (PG) optical survey of quasars covers nearly the same area of the sky covered by the IRAS Bright Galaxy Survey. A search of the PG list of bright quasars (Schmidt and Green 1983) for objects in the same redshift range as the ultraluminous infrared galaxies yields only five quasars—Ton 951, Ton 1542, I Zw 1, II Zw 136, and Mrk 478—all of which have bolometric luminosities in the range log $(L_{bol}/L_\odot) = 12.0$–12.5. None of these quasars has a bolometric luminosity larger than that of Mrk 231. A more accurate comparison of space densities by Soifer et al. (1986), comparing the bolometric luminosities of PG quasars and infrared galaxies, shows that there are actually ∼3.5 times
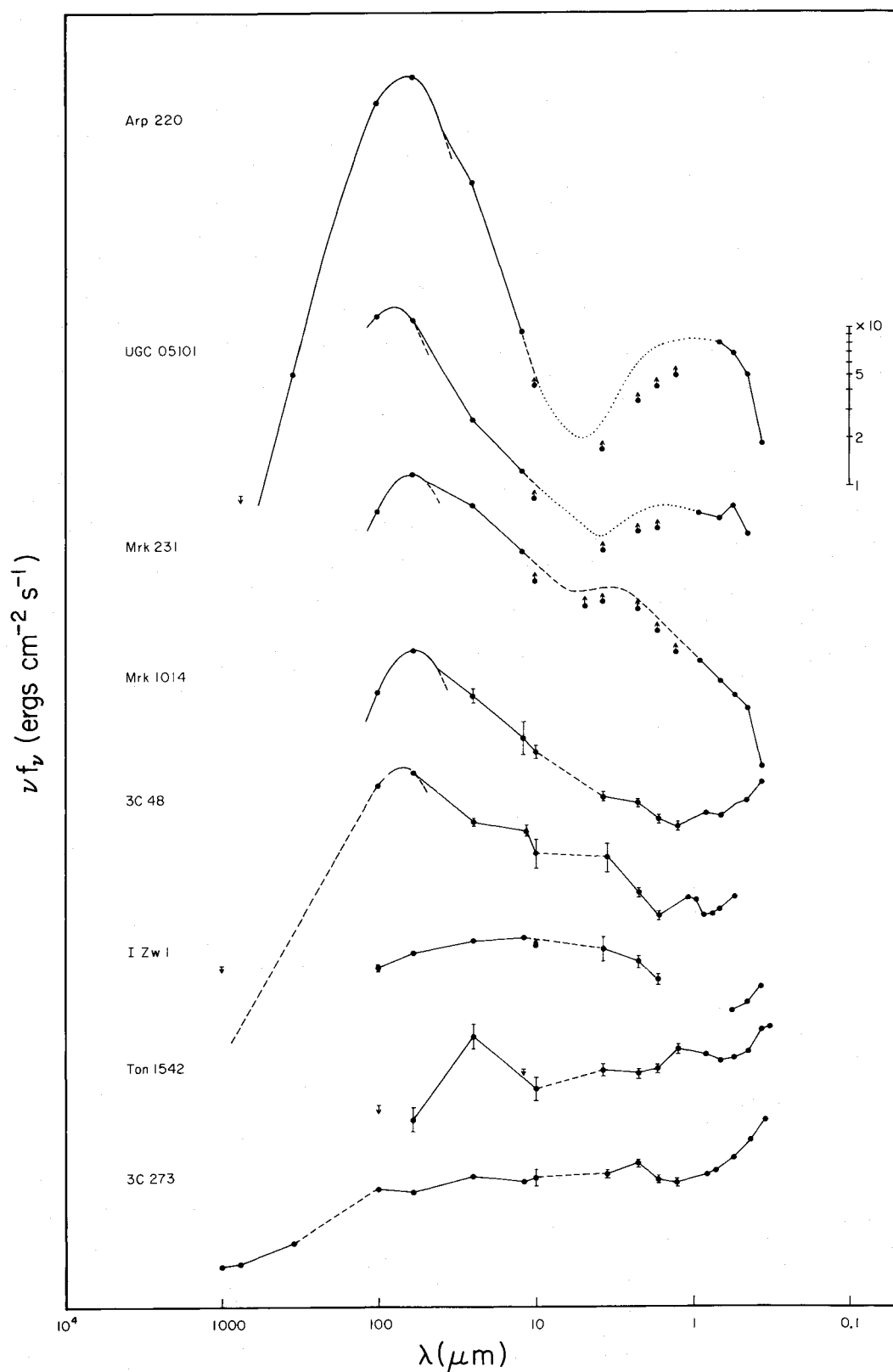
FIG. 17.—Spectral energy distributions for selected ultraluminous infrared galaxies and quasars which illustrate the proposed spectral evolution (see text) from the infrared extreme objects like Arp 220 to the relatively unobscured quasars like Ton 1542 and 3C 273. Data for 3C 48 and 3C 273 are from Neugebauer, Soifer, and Miley (1985). For 3C 48 the dashed line connects the measured 100 μm data point to the highest frequency measurement (not shown) in the radio. The optical and near-infrared data for the other objects, as well as the *IRAS* data for Mrk 1014, are from Neugebauer *et al.* (1986, 1987*a*).

as many infrared galaxies per unit volume as optical quasars in the range $\log (L_{bol}/L_\odot) = 12.0$–$12.5$.

There is substantial evidence suggesting that interactions play a role in triggering quasars. Imaging surveys of quasars in the optical continuum show that $\sim 30\%$ of the low-redshift ($z \lesssim 0.4$) quasars have close companions and/or appear distorted (see review by Hutchings 1983). However these surveys would not have been able to detect the relatively faint tails and distortions observed in the majority of the ultraluminous infrared galaxies, particularly in the case of an advanced merger. Therefore, a much larger fraction, perhaps all of the optical quasars, could be the result of strong galaxy interactions. More direct evidence that mergers may be responsible for the majority of quasars comes from the imaging of several quasars in the [O III] line (Stockton and MacKenty 1983; MacKenty and Stockton 1984; Shara, Moffet, and Albrecht 1985). These observations show that the quasar host galaxy appears to be an advanced merger as evidenced by tidal tails extending from a still unresolved (presumably completely merged) parent body. It should also be noted that Vader *et al.* (1987) claim that the infrared-loud quasar *IRAS* 00275−2859 resides in a merging galaxy system.

There is limited, but convincing, evidence from studies of local quasars that they reside in gas-rich spirals. Recent measurements have been made of the H I gas content of all of the nearby quasars by Condon, Hutchings, and Gower (1985). They find H I masses *typical of large spirals.* CO(1 → 0) measurements, which would allow a determination of the mass of molecular gas, have not been made. It might be expected that the molecular gas is disrupted or destroyed by the time such systems appear as UV-excess quasars.

From the above morphological evidence alone it is possible to make a conclusive case for the origin of quasars from galaxy interactions (Bothun *et al.* 1982; Stockton 1982; Hutchings, Crampton, and Campbell 1984; Yee and Green 1984; De Robertis 1985). The new data for ultraluminous infrared galaxies would seem to enhance greatly this picture by providing a parent population of strongly interacting galaxies, sufficient in number and luminosity to account for the observed number of local quasars.

b) Formation of Ultraluminous Infrared Galaxies at Earlier Epochs

The ultraluminous infrared galaxies from the Bright Galaxy Survey have luminosities and space densities similar to those of quasars in the local universe. However, at larger redshifts, quasars have much greater space densities and luminosities (although there is less than a factor of ~ 80 needed to account for the most luminous quasars). Do ultraluminous infrared galaxies exist with luminosities and space densities high enough to account for the high redshift quasars? While data on ultraluminous infrared galaxies at $z = 2$ do not exist, observations of *IRAS* sources at lower redshift (Kleinmann and Keel 1987; Vader and Simon 1987; Neugebauer, Soifer, and Miley 1985) show that infrared luminous objects with luminosities in excess of $10^{13} L_\odot$ can be found at $z \leq 0.5$ in reasonable numbers.

Similar evolution to that of the optical quasars is *expected* for ultraluminous infrared galaxies, since galaxy collisions provide a natural explanation of the increased density of quasars at earlier epochs when the universe was smaller and collisions more frequent. This fact, combined with an expected increase in gas supplies in galaxy disks could account for the observed evolution in the quasar luminosity function (e.g., Schmidt and Green 1983).

Preliminary indications that evolution does exist in the number counts of faint *IRAS* galaxies has recently been provided by Hacking, Condon, and Houck (1987). Further observations of ultraluminous *IRAS* galaxies at faint flux levels would be extremely important in establishing a firmer evolutionary link between infrared galaxies and optical quasars.

VI. SUMMARY

Observations of a complete sample of 10 ultraluminous infrared galaxies show that (1) all are strongly interacting galaxies—most appear to be advanced mergers of two spiral disks, (2) nine of 10 have dominant nonthermal optical emission lines, (3) the near-infrared colors show a mixture of starburst and AGN energy sources, and (4) all appear to be extremely rich in molecular gas. These observations have been interpreted to imply that the ultraluminous infrared objects are, in fact, dust-enshrouded quasars.

A model has been presented for the formation of ultraluminous infrared galaxies through the strong interaction, or merger of two molecular gas-rich spirals. The funneling of molecular gas clouds toward a merger nucleus accounts for both a nuclear starburst and provides fuel in the form of gas and stellar remnants for an active nucleus. In the ultraluminous infrared phase it is assumed that the active nucleus dominates the starburst which may already have begun to fade. Once the combined forces of radiation pressure and supernovae explosions begin to sweep dust clear of the nuclear region these objects will take on the appearance of optical quasars. Current observations of quasars and infrared galaxies in the local universe are consistent with the idea that the majority of quasars are formed through galaxy collisions and that all quasars may start in an ultraluminous infrared phase.

APPENDIX A

THE ULTRALUMINOUS INFRARED GALAXY SAMPLE—OPTICAL MORPHOLOGY

The descriptions below are based primarily on the optical images obtained with the Palomar 5 m and 1.5 m telescopes (Figs. 2–11). Quoted sizes and distances have been computed from the object redshift given in Table 1 assuming $H_0 = 75 \text{ km s}^{-1} \text{ Mpc}^{-1}$.

IRAS 05189−2524.—This is the only object which appears "principally stellar" on the POSS. A deep exposure on the Palomar 1.5 m telescope was required to reveal the 30″ disk shown in Figure 1. In addition, two crossed tails are revealed, leading us to identify this object as an advanced merger of two spiral disks. The slightly curved tails extend from the midpoint of the disk's western edge. At a redshift of 0.040 the larger northern tail is ∼40 kpc in length.

IRAS 08572+3915.—The "L-shaped" appearance of this object on the POSS suggested that it was composed of two overlapping spirals. The CCD image confirms this interpretation and also shows two nuclei separated by ∼4 kpc. Infrared photometry indicates that nearly all of the 10 μm flux comes from the northwest nucleus.

IRAS 09320+6134 = UGC 05101 = MCG +10-14-025 = Zw 289.011.—This is a "distinctly peculiar" object on the POSS, with a 15 kpc straight jet extending to the west and a large ring. In addition, the CCD image shows a single bright nucleus and an assortment of smaller wisps or tails interior to the ring. Ring galaxies are thought to be formed from penetrating collisions of near face-on disks; however there is no obvious intruder galaxy in this system. Either the two nuclei have merged or the intruder nucleus is hidden behind the bright nucleus and jet.

IRAS 12112+0305.—This object appears to be two interacting spiral galaxies on the POSS. CCD images show a double nucleus separated by less than 3 kpc, the northern nucleus being much brighter than the southern. The two spirals both appear to be nearly edge-on.

IRAS 12540+5708 = A1254+57 = UGC 08058 = Markarian 231 (misidentified as Markarian 230 in the UGC) = MCG +10-19-004 = VII Zw 490.—Since the early, near-infrared observations of Young, Knacke, and Joyce (1972) and Rieke and Low (1972), this object has been known to be extremely luminous in the infrared. Our results show that it is the most luminous infrared object in the local universe ($z \lesssim 0.1$). The trigger for this object's extreme luminosity has been discussed in two recent independent studies by Sanders *et al.* (1987*a*), and Hutchings and Neff (1987). The deep CCD images obtained by these two groups clearly show two striking tidal tails extending north-south from the eastern edge of the nearly completely merged spiral disks. The image shown in Figure 6 is taken from Sanders *et al.* (1987*a*).

IRAS 13428+5608 = A1342+56 = UGC 08696 = Markarian 273 = MCG +09-23-004 = I Zw 71 = VV 851.—Like Markarian 231, this galaxy has been known for some time to be extremely luminous in the near-infrared. Markarian (1969) described it as an "exceedingly interesting galaxy with large straight protrusion." It has since been characterized as a double nucleus (Wehinger and Wyckoff 1977) or a triple-nucleus system (Korovyakovskii *et al.* 1981). The straight protrusion, or jet, is ∼20 kpc long. Figures 7 and 1 clearly show these structures. In addition, our current work identifies the starlike blue object ∼40″ north of the main body of Mrk 273 as a galaxy whose redshift is only 50 km s^{-1} different from that of Mrk 273. This galaxy is on a direct line with the Mrk 273 "jet." The highly distorted disk of Mrk 273 is actually composed of one extremely bright Seyfert nucleus, presumably the original nucleus of Mrk 273, and two lesser blobs which are most likely major clumps of star formation. The northern companion has a strong H II region–like, emission-line spectrum.

IRAS 14348−1447.—The POSS image shows two straight tails extending in opposite directions from a pear-shaped object less than 20″ in size. With a redshift of 0.081 this is the most distant object in the *IRAS* Bright Galaxy Sample. The CCD image shows two nuclei separated by about 4 kpc.

IRAS 15250+3609.—The POSS image suggests a ring galaxy, but with an additional jet feature, similar to one of the several such structures seen in *IRAS* 09320+6134. However, unlike the latter there are several small companion galaxies close to the ring. The companion north of the bright nucleus, and just outside the ring, may be the intruder galaxy responsible for the observed havoc. Alternatively, another galaxy may have embedded itself in the nuclear region of the larger system, its disk now forming the eastern protrusion extending from the bright nucleus.

IRAS 15327+2340 = IC 4553+4554 = UGC 09913 = MCG +04-37-005 = Zw 136.017 = Arp 220 = K470A.—This object was highlighted by Soifer *et al.* (1984*b*), during the initial phase of the *IRAS* data analysis, as having the highest ratio of infrared-to-blue luminosity of any previously cataloged galaxy. At that time there was still considerable uncertainty about the nature of the host galaxy. The apparent double optical nucleus (i.e., UGC 09913 = IC 4553 and IC 4554, Nilson 1973), as shown in Figure 10, is now known from near-infrared (Neugebauer *et al.* 1987*b*) and radio-continuum measurements to be either a single or <1″ double nucleus crossed by a dust lane. The optical image shown in Figures 10 and 1 clearly indicates that Arp 220 is a merger system. Two large (total extent ∼35 kpc at a redshift of 0.018), but relatively faint, crossed tidal tails extend from the midpoint of the western edge of the merged disks.

IRAS 22491−1808.—Even though this object is the next most distant of the ultraluminous galaxies, it was one of the clearest merger systems on the POSS. The "boomerang" shape is caused by two thick tails extending from a distorted central body ∼15 kpc in diameter.

REFERENCES

Aaronson, M. 1977, Ph.D. thesis, Harvard University.
Becklin, E. E., and Wynn-Williams, C. G. 1987, in *Star Formation in Galaxies*, ed. C. J. Persson (Washington, DC: U.S. Government Printing Office), p. 643.
Beichman, C. A., Soifer, B. T., Helou, G., Chester, T. J., Neugebauer, G., Gillett, F. C., and Low, F. J. 1986, *Ap. J. (Letters)*, **308**, L1.
Bothun, G. D., Mould, J., Heckman, T., Balick, B., Schommer, R. A., and Kristian, J. 1982, *A.J.*, **87**, 1621.
Carico, D. P., Soifer, B. T., Elias, J. H., Matthews, K., Neugebauer, G., and Beichman, C. 1986, *A.J.*, **92**, 1254.

Cataloged Galaxies and Quasars Detected in the IRAS Survey. 1985, prepared by C. J. Persson, G. Helou, J. C. Good, and W. L. Rice, JPL D1932 (internal document).
Condon, J. J., Hutchings, J. B., and Gower, A. L. 1985, *A.J.*, **90**, 1642.
deGrijp, M. H. K., Miley, G. K., and Lub, J. 1987, preprint.
Depoy, D. L. 1987, in *Star Formation in Galaxies*, ed. C. J. Persson (Washington, DC: US Government Printing Office), p. 701.
De Robertis, M. M. 1985, *A.J.*, **90**, 998.
Elston, R., Cornell, M. E., and Lebofsky, M. J. 1985, *Ap. J.*, **296**, 106.

Emerson, J. P., Clegg, P. E., Gee, G., Cunningham, C. T., Griffin, M. J., Brown, L. M. J., Robson, E. I., and Longmore, A. J. 1984, *Nature*, **311**, 237.
Filippenko, A., and Sargent, W. L. W. 1985, *Ap. J. Suppl.*, **57**, 503.
French, H. B. 1980, *Ap. J.*, **240**, 41.
Hacking, P., Condon, J. J., and Houck, J. R. 1987, *Ap. J. (Letters)*, **316**, L15.
Harwit, M. O., Houck, J. R., Soifer, B. T., and Palumbo, G. G. C. 1987, *Ap. J.*, **315**, 28.
Heckman, T. M., van Breugel, W., Miley, G. K., and Butcher, H. R. 1983, *A.J.*, **88**, 1077.
Houck, J. R., *et al.* 1984, *Ap. J. (Letters)*, **278**, L63.
Houck, J. R., Schneider, D. P., Danielson, G. E., Beichman, C. A., Lonsdale, C. J., Neugebauer, G., and Soifer, B. T. 1985, *Ap. J. (Letters)*, **290**, L5.
Hutchings, J. B. 1983, *Pub. A.S.P.*, **95**, 799.
Hutchings, J. B., Crampton, D., and Campbell, B. 1984, *Ap. J.*, **280**, 41.
Hutchings, J. B., and Neff, S. G. 1987, *A.J.*, **93**, 14.
IRAS Point Source Catalog, 1985 (Washington, DC: US Government Printing Office) (PSC).
Joy, M., Lester, D. F., Harvey, P. M., and French, M. 1986, *Ap. J.*, **307**, 110.
Khachikian, E. Ye., and Weedman, D. W. 1974, *Ap. J.*, **192**, 581.
Kleinmann, S. G., and Keel, W. C. 1987, in *Star Formation in Galaxies*, ed. C. J. Persson (Washington, DC: US Government Printing Office), p. 559.
Korovyakovskii, Y. P., Petrosyan, A. R., Saakyan, K. A., and Khachikyan, E. E. 1981, *Astrofizika*, **17**, 231.
Lawrence, A., Walker, D., Rowan-Robinson, M., Leech, K. J., and Penston, M. V. 1986, *M.N.R.A.S.*, **219**, 687.
Lynds, C. R., and Toomre, A. 1976, *Ap. J.*, **209**, 382.
MacKenty, J. W., and Stockton, A. 1984, *Ap. J.*, **283**, 64.
Markarian, B. E. 1969, *Astrofizika*, **5**, 581.
Matthews, K., Neugebauer, G., McGill, J., and Soifer, B. T. 1987, *A.J.*, **94**, 297.
Miley, G. K., Neugebauer, G., and Soifer, B. T. 1985, *Ap. J. (Letters)*, **293**, L11.
Neugebauer, G., Green, R. J., Matthews, K., Schmidt, M., Soifer, B. T., and Bennett, J., 1987a, *Ap. J. Suppl.*, **63**, 615.
Neugebauer, G., Elias, J. H., Matthews, K., McGill, J., Scoville, N. Z., and Soifer, B. T. 1987b, *A.J.*, **93**, 1097.
Neugebauer, G., Matthews, K., Soifer, B. T., and Elias, J. H. 1985, *Ap. J.*, **298**, 275.
Neugebauer, G., Miley, G. K., Soifer, B. T., and Clegg, P. E. 1986, *Ap. J.*, **308**, 815.
Neugebauer, G., Soifer, B. T., and Miley, G. K. 1985, *Ap. J. (Letters)*, **295**, L27.
Nilson, P. 1973, *Uppsala General Catalogue of Galaxies* (*Acta Universitatis Upsaliensis, Nova Regiae Societatis Scientiarum Upsaliensis*) Series V: A, Vol. **1** (UGC).
Oke, J. B., and Gunn, J. E. 1982, *Pub. A.S.P.*, **94**, 586.
Osterbrock, D. E. 1984, *Quart. J.R.A.S.*, **18**, 1.
Perault, M., Boulanger, F., Falgarone, E., and Puget, J. L. 1986, *Astr. Ap.*, submitted.
Rieke, G. H., and Low, F. J. 1972, *Ap. J. (Letters)*, **176**, L95.
Sanders, D. B., and Mirabel, I. F. 1985, *Ap. J. (Letters)*, **298**, L31.

Sanders, D. B., Scoville, N. Z., and Soifer, B. T. 1988, *Ap. J.*, submitted.
Sanders, D. B., Scoville, N. Z., and Solomon, P. M. 1985, *Ap. J.*, **276**, 182.
Sanders, D. B., Scoville, N. Z., Young, J. S., Soifer, B. T., Schloerb, F. P., Rice, W. L., and Danielson, G. E. 1986, *Ap. J. (Letters)*, **305**, L45.
Sanders, D. B., Solomon, P. M., and Scoville, N. Z. 1984, *Ap. J.*, **276**, 182.
Sanders, D. B., Young, J. S., Scoville, N. Z., Soifer, B. T., and Danielson, G. E. 1987a, *Ap. J. (Letters)*, **312**, L5.
Sanders, D. B., *et al.* 1987b, in *Star Formation in Galaxies*, ed. C. J. Persson (Washington, DC: US Government Printing Office), p. 411.
Sanders, D. B., *et al.* 1987c, in preparation.
Schmidt, M., and Green, R. F. 1983, *Ap. J.*, **269**, 352.
Scoville, N. Z., and Good, J. 1987, in *Star Formation in Galaxies*, ed. C. J. Persson (Washington, DC: US Government Printing Office), p. 3.
Scoville, N. Z., Sanders, D. B., and Clemens, D. P. 1986, *Ap. J. (Letters)*, **310**, L77.
Scoville, N. Z., Sanders, D. B., Sargent, A. I., Soifer, B. T., Scott, S. L., and Lo, K. Y. 1986, *Ap. J. (Letters)*, **311**, L47.
Shara, M. M., Moffet, A. F. T., and Albrecht, R. 1985, *Ap. J.*, **296**, 399.
Soifer, B. T., Sanders, D. B., Madore, B. F., Neugebauer, G., Persson, C. J., Persson, S. E., and Rice, W. L. 1987, *Ap. J.*, **320**, 238.
Soifer, B. T., Sanders, D. B., Neugebauer, G., Danielson, G. E., Lonsdale, C. J., Madore, B. F., and Persson, S. E. 1986, *Ap. J. (Letters)*, **303**, L41.
Soifer, B. T., *et al.* 1984a, *Ap. J. (Letters)*, **278**, L71.
———. 1984b, *Ap. J. (Letters)*, **283**, L1.
Solomon, P. M., Rivolo, A. R., Mooney, T. J., Barrett, J. W., and Sage, L. J. 1987, in *Star Formation in Galaxies*, ed. C. J. Persson (Washington, DC: US Government Printing Office), p. 37.
Stockton, A. 1982, *Ap. J.*, **257**, 33.
Stockton, A., and MacKenty, J. W. 1983, *Nature*, **305**, 678.
Toomre, A. 1964, *Ap. J.*, **139**, 1217.
———. 1977, in *Evolution of Galaxies and Stellar Populations*, ed. R. B. Larson and B. M. Tinsley (New Haven: Yale Observatory Press), p. 401.
Toomre, A., and Toomre, J. 1972, *Ap. J.*, **178**, 623.
Vader, J. P., Da Costa, G. S., Frogel, J. A., Heisler, C. A., and Simon, M. 1987, preprint.
Vader, J. P., and Simon, M. 1987, *Nature*, **327**, 304.
Veilleux, S., and Osterbrock, D. E. 1987, *Ap. J. Suppl.*, **63**, 295.
Véron-Cetty, M.-P., and Véron, P. 1985, *ESO Sci. Rept., No. 4*.
Weedman, D. W. 1983, *Ap. J.*, **243**, 756.
Wehinger, P. A., and Wyckoff, S. 1977, *M.N.R.A.S.*, **181**, 211.
Yee, H. K. C., and Green, R. F. 1984, *Ap. J.*, **280**, 79.
Young, E. T., Knacke, R. F., and Joyce, R. R. 1972, *Nature*, **238**, 263.
Young, J. S. 1986, in *IAU Symposium 115, Star Formation*, ed. M. Peimbert and J. Jungaku (Dordrecht: Reidel), in press.
Young, J. S., Kenney, J., Lord, S., and Schloerb, F. P. 1984, *Ap. J. (Letters)*, **287**, L65.

J. H. Elias: CTIO, Casilla 603, La Serena, Chile

B. F. Madore, K. Matthews, G. Neugebauer, D. B. Sanders, and B. T. Soifer: California Institute of Technology, Downs Lab, 320-47, Pasadena, CA 91125

N. Z. Scoville: California Institute of Technology, Robinson, 105-24, Pasadena, CA 91125